

**SYNTHESIS AND CHARACTERIZATION OF WATER-SOLUBLE RUTHENIUM
PORPHYRIN COMPLEXES AS RADIOSENSITIZERS**

by

Caroline Jane Ware

B. Sc. (Hons), University of Dundee, 1992

A thesis submitted in partial fulfillment
of the requirements for the degree of
Master of Science in
THE FACULTY OF GRADUATE STUDIES
(Department of Chemistry)

We accept this thesis as conforming
to the required standard

THE UNIVERSITY OF BRITISH COLUMBIA

December 1994

© C. J. Ware, 1994

In presenting this thesis in partial fulfilment of the requirements for an advanced degree at the University of British Columbia, I agree that the Library shall make it freely available for reference and study. I further agree that permission for extensive copying of this thesis for scholarly purposes may be granted by the head of my department or by his or her representatives. It is understood that copying or publication of this thesis for financial gain shall not be allowed without my written permission.

Department of

Chemistry

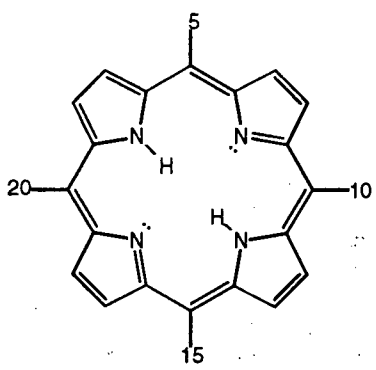
The University of British Columbia
Vancouver, Canada

Date

6/2/95

Abstract

The coordination chemistry of Ru in conjunction with the water-soluble porphyrins, $\text{H}_2(\text{TSPP})^{4-}$ and $\text{H}_2(\text{TMPyP})^{4+}$, and the non water-soluble porphyrins $\text{H}_2(\text{TPyP})$ and $\text{H}_2(\text{TPP})$ was examined with the view of producing a range of complexes with radiosensitizing abilities for the treatment of cancerous tumours. The new complex $\text{Na}_4[\text{Ru}(\text{TSPP})(\text{CO})(\text{DMF})]$ (**1**) (DMF = dimethylformamide) was synthesized by thermolysis of $\text{Ru}_3(\text{CO})_{12}$ with the porphyrin salt in DMF, and by a more convenient route involving the Ru(III) precursor, $[\text{Ru}(\text{DMF})_6](\text{OTf})_3$ (OTf = triflate), which undergoes *in situ* reduction in DMF in the presence of $\text{H}_2(\text{TSPP})^{4-}$ to give **1**. This hexakis(DMF) precursor also allows metallation of $\text{H}_2(\text{TMPyP})^{4+}$, $\text{H}_2(\text{TPyP})$, and $\text{H}_2(\text{TPP})$, establishing a protocol for the metallation by Ru of cationic, anionic, and neutral porphyrins. Various other strategies for porphyrin metallation by ruthenium were examined without success.

Porphyrin Structure	Full name (abbreviation)
	5, 10, 15, 20-tetraphenylporphyrin ($\text{H}_2(\text{TPP})$)
	5, 10, 15, 20-tetra(4-pyridyl)porphyrin ($\text{H}_2(\text{TPyP})$)
	5, 10, 15, 20-tetrakis(4-sulfonatophenyl)porphyrin ($\text{H}_2(\text{TSPP})^{4-}$)
	5, 10, 15, 20-tetrakis(4-methylpyridinium)porphyrin ($\text{H}_2(\text{TMPyP})^{4+}$)

Complex **1** was well characterized by variable temperature ^1H and $^{13}\text{C}\{^1\text{H}\}$ NMR, IR, and UV/visible spectroscopy, and by elemental analysis. **1** undergoes photolysis or thermolysis in DMSO to give the second new metalloporphyrin $\text{Na}_4[\text{Ru}(\text{TSPP})(\text{DMSO})_2]$ (**2**) (DMSO = dimethylsulphoxide) by removal of the axial CO and DMF groups. The ^1H NMR

spectrum in d_6 -DMSO of **2** is consistent with a symmetric, D_{4h} structure, and the solid-state IR spectrum indicates coordination by the oxygen atoms of the DMSO ligands. The axial ligand exchange that **2** undergoes in aqueous solution, examined by UV/visible spectroscopy, is believed to involve the replacement of DMSO by water.

For both **1** and **2** the degree of aggregation in aqueous solution over a concentration range of 10^{-6} - 10^{-4} mol L⁻¹ was assessed by UV/visible spectroscopy; Beer's Law behaviour precludes significant aggregation phenomenon.

Complexes **1** and **2** were assessed for their biological activity by accumulation, toxicity, DNA binding, and radiosensitization studies. **1** accumulates in Chinese Hamster Ovary cells (CHO), and shows no signs of toxicity toward CHO cells up to 200 μ molar concentrations. Relative to *Cis*-platin, **1** and **2** display marginal binding to plasmid DNA, and on binding do not form associations with High Mobility Group proteins (HMG). **2** was weakly radio-protecting in hypoxic conditions at 400 and 800 μ molar concentrations.

Table of Contents

	Page
Abstract	ii
Table of Contents	iv
List of Figures	viii
List of Tables	ix
General Abbreviations	x
List of abbreviations of porphyrins and metalloporphyrins that appear in this work	xii
A. Free-base porphyrins.	xii
B. Ru metalloporphyrins.	xiii
Acknowledgements	xiv
 Chapter 1: Introduction	 1
1.1 Preamble.....	1
1.2 Cancer Treatment	2
1.2.1 Surgery	2
1.2.2 Radiotherapy	2
1.2.3 Chemotherapy	3
1.3 Effects of Radiation	4
1.3.1 Radiation-induced DNA damage	4
1.3.2 Radiolysis of water.....	5
1.3.3 Damage fixation by oxygen	7
1.3.4 The oxygen effect.....	7
1.3.5 Hypoxia	9

1.4 Radiosensitizers	9
1.5 Radiosensitizer Drug Design	10
1.5.1 Tumour accumulation and localization	10
1.5.2 DNA binders	11
1.5.3 Metalloporphyrin complexes	12
1.6 The Scope of the Thesis	12
1.7 References	13

Chapter 2: Experimental Section for the Synthetic Inorganic and Organic

Chemistry	18
2.1 Reagents	18
2.2 Physical Techniques and Methods	18
2.3 Syntheses of the Free-Base Porphyrins	19
2.3.1 Syntheses of $H_2(TPP)$, $H_2(TPyP)$ and $H_2(TMPyP)^{4+}$	19
2.3.2 Synthesis of $Na_4[H_2(TSPP)]$	20
2.4 Preparation of the Ruthenium Precursor Complexes	21
2.4.1 $Ru_3(CO)_{12}$	21
2.4.2 $Cis-RuCl_2(DMSO)_4$	21
2.4.3 $[Ru(DMF)_6](OTf)_3$	21
2.5 Metallation Reactions	22
2.5.1 Synthesis of $Na_4[Ru(TSPP)(CO)(DMF)]$ (1)	22
2.5.2 Reaction of $[Ru(DMF)_6](OTf)_3$ with $H_2(TPyP)$	24
2.5.3 Reaction of $[Ru(DMF)_6](OTf)_3$ with $H_2(TMPyP)^{4+}$	24
2.5.4 Reaction of $[Ru(DMF)_6](OTf)_3$ with $H_2(TPP)$	25
2.6 Synthesis of $Na_4[Ru(TSPP)(DMSO)_2]$ (2)	25
2.7 References	28

Chapter 3: Results and Discussion	29
3.1 General Background	29
3.2 Ruthenium Metalloporphyrins	30
3.3 Syntheses of Water-Soluble Ru Porphyrins.....	31
3.3.1 Ru ₃ (CO) ₁₂ precursor.....	31
3.3.2 <i>Cis</i> -RuCl ₂ (DMSO) ₄ and [Ru(DMF) ₆](OTf) ₃ precursors	32
3.4 Structure of Na ₄ [Ru(TSPP)(CO)(DMF)] (1)	35
3.5 Other Ruthenium Porphyrins	39
3.6 Removal of the Axial CO Group from Ru(TSPP)(CO)(DMF) ⁴⁻ (1)	40
3.6.1 Photolysis of 1	40
3.6.2 Thermolysis of 1	42
3.7 Aggregation Studies.....	42
3.7.1 Axial ligand substitution promoting aggregation/disaggregation	47
3.8 References	51
 Chapter 4: Biological Tests	 54
4.1 Introduction	54
4.2 Cell Preparation.....	54
4.3 Cell Accumulation	55
4.3.1 Accumulation study of 1	55
4.4 Toxicity	56
4.2.1 Toxicity of 1 toward CHO cells.....	57
4.4 DNA Binding	58
4.4.1 Plasmid binding.....	58
4.4.1.1 Electrophoresis gels	59
4.4.2 The Damaged DNA Affinity Precipitation Assay (DDAP)	60
4.4.2.1 Results of the damaged DNA precipitation	62
4.5 Radiosensitization	62

4.5.1 The radiosensitizing ability of 2	63
4.6 References	65
Chapter 5: Conclusions and Suggestions for Future Work	66
5.1 Retrospective.....	66
5.2 Prospective	67
5.3 References	69
Appendix I: Infrared Spectrum (KBr disc) of Complex 1	70
Appendix II: $^{13}\text{C}\{^1\text{H}\}$ NMR Spectrum of $\text{Ru}(\text{TSPP})(^{13}\text{CO})(\text{DMF})_4^-$	71
Appendix III: Solutions Used for the Biological Tests.	72

List of Figures

	Page
Figure 1.1:	4
Diagram (from Hall) illustrating direct and indirect action of radiation. The structure of DNA is shown schematically; the letters S, P, A, T, G, and C represent sugar, phosphate, adenine, thymine, guanine, and cytosine, respectively.	
Figure 1.2:	8
A typical survival curve for Chinese Hamster Ovary (CHO) cells as a function of radiation dose.	
Figure 3.1:	29
Generalized porphyrin structure.	
Figure 3.2:	31
Water-soluble porphyrins.	
Figure 3.3:	36
Variable temperature ^1H NMR of $\text{Na}_4[\text{Ru}(\text{TSPP})(\text{CO})(\text{DMF})]\cdot 2\text{DMF}\cdot 2\text{H}_2\text{O}$ (1) in d_6 -DMSO; the doublets (d) and triplet (t) assignments are described in the text. This is a stacked plot and does not represent a change in chemical shift with temperature. The signals marked with an asterisk correspond to small amounts of the thermolysis product $\text{Ru}(\text{TSPP})(\text{DMSO})_2^{4-}$ (see Sections 2.6 (b) and 3.6.2).	
Figure 3.4:	35
Different chemical environments for the phenyl protons in 1 .	
Figure 3.5:	42
Canonical forms of DMSO.	
Figure 3.6:	44-45
Beer's Law study of A: complex 1 , B: complex 2 , and C: $\text{H}_2(\text{TSPP})^{4-}$, in aqueous solution over a concentration range of 10^{-6} - 10^{-4} mol L $^{-1}$ in 0.1 cm and 1 cm cells.	
Figure 3.7:	46
Aggregation study of 1 and 2 (concentration = 2.0×10^{-5} mol L $^{-1}$)	
Figure 3.8:	48
Soret band absorption change when 2 is heated in aqueous solution.	

Figure 3.9:	Soret band absorption change upon the addition of DMSO.	49
Figure 3.10:	Q band absorption change when 2 is heated in aqueous solution (due to technical difficulties the final spectrum at $\lambda_{\text{max}} = 526 \text{ nm}$ could not be overlayed onto the graph).	50
Figure 4.1:	Accumulation of Ru from incubation of CHO cells with 1 (50 - 200 $\mu\text{mol L}^{-1}$) for 1 hour.	56
Figure 4.2:	Toxicity study of complex 1 (50 - 200 $\mu\text{mol L}^{-1}$) in CHO cells (oxic conditions).	58
Figure 4.3:	DNA binding study of 1 and 2 at or near the BamH1 binding sites of the plasmid DNA.	60
Figure 4.4:	Survival curve for radiosensitizing by 2 in oxic and hypoxic cells.	64

List of Tables

Table 2.1:	UV/visible data for the free-base porphyrins and the ruthenium(II) porphyrins.	27
------------	--	----

General Abbreviations

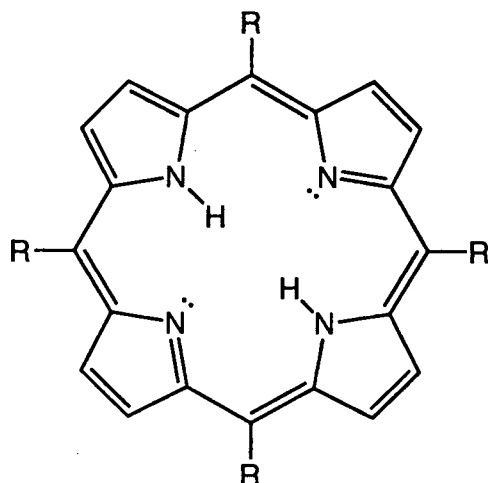
The following abbreviations, most of which are commonly found in the literature, are used in this thesis.

Å	Angstrom (10^{-10}m).
AA	Atomic absorption.
AAS	Atomic absorption spectroscopy.
anal.	analysis.
APT	Attached Proton Test.
br	broad.
° C	degree Celsius.
calcd	calculated.
CHO	Chinese Hamster Ovary (cell line).
δ	chemical shift (NMR).
DMF	Dimethylformamide.
DMSO	Dimethylsulfoxide.
ϵ	Molar absorptivity.
H ₄ EDTA	Ethylenediaminetetraacetic acid.
eq	equation.
Et	Ethyl, $-\text{C}_2\text{H}_5$.
eV	electron volts.
Gy	Gray = 100 rads.
HSAB	Hard Soft Acid Base Principle.
Hz	Hertz.
ⁱ Pr	Isopropyl, $-\text{CH}(\text{CH}_3)_2$.
IR	Infrared.
<i>J</i>	scalar nuclear spin-spin coupling constant (NMR).

kV	kilo volts.
L	Litre (s).
λ	wavelength (nm).
<i>m</i>	<i>meta</i> .
m	multiplet (NMR).
Me	Methyl, CH ₃ .
min	minute.
mL	millilitre.
μm	micrometer.
mol	mole (s).
v	wavenumber, cm ⁻¹ .
NMR	Nuclear Magnetic Resonance.
<i>o</i>	<i>ortho</i> .
OTf	Triflate, CF ₃ SO ₃ ⁻ .
<i>p</i>	<i>para</i> .
Ph	Phenyl.
ppm	parts per million.
R	hydrocarbyl substituent.
rads	energy of absorption of 100 ergs/g.
rpm	revolutions per minute.
s	singlet (NMR).
THF	Tetrahydrofuran.
UV	Ultra-violet.

List of abbreviations of porphyrins and metalloporphyrins that appear in this work

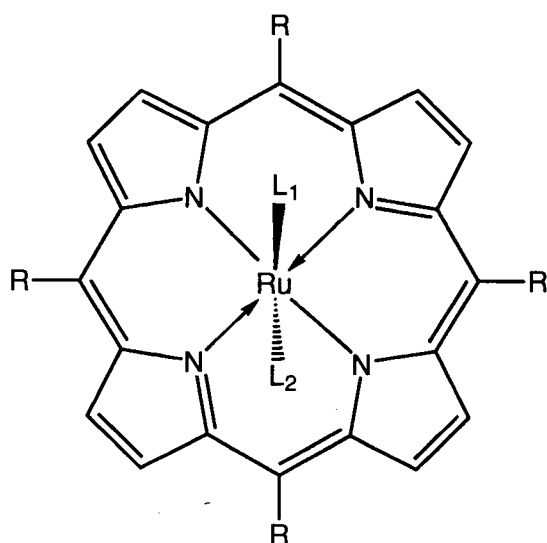
A. Free-base porphyrins.



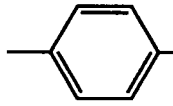
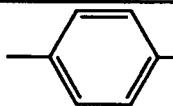
The generalized porphyrin structure is depicted in the adjoining figure. The abbreviations for the porphyrins used in this thesis appear in the table below.

Full name	Abbreviation	R group
5, 10, 15, 20-tetraphenyl porphyrin	H ₂ (TPP)	
5, 10, 15, 20-tetra(4-pyridyl) porphyrin	H ₂ (TPyP)	
5, 10, 15, 20-tetrakis(4-sulfonatophenyl)porphyrin	H ₂ (TSPP) ⁴⁻	
5, 10, 15, 20-tetrakis(4-methylpyridinium)porphyrin	H ₂ (TMPyP) ⁴⁺	

B. Ru metalloporphyrins.



The generalized Ru metalloporphyrin complex is depicted in the adjoining figure. Ru porphyrin complexes synthesized in this work and abbreviations used appear in the following table.

Full name	Abbreviation	R group
(5, 10, 15, 20-tetrakis(4-sulfonatophenyl)porphyrinato) carbonyl(dimethylformamide) ruthenate(II) (1)	$\text{Ru}(\text{TSPP})(\text{CO})(\text{DMF})^{4-}$	 $\text{L}_1 = \text{CO}$ $\text{L}_2 = \text{DMF}$
(5, 10, 15, 20-tetrakis(4-sulfonatophenyl)porphyrinato) bis(dimethylsulfoxide) ruthenate(II) (2)	$\text{Ru}(\text{TSPP})(\text{DMSO})_2^{4-}$	 $\text{L}_1 = \text{DMSO}$ $\text{L}_2 = \text{DMSO}$

Also synthesized but incompletely characterized were:

- “Ru(TPyP)” R = 4-pyridyl; the nature of the axial ligands is unknown;
 “Ru(TMPyP)” R = 4-methylpyridinium; the nature of the axial ligands is unknown;
 “Ru(TPyP)” R = phenyl; the nature of the axial ligands is unknown.

Acknowledgements

I would like to express my sincere gratitude to my research supervisors Dr. Brian James and Dr. Kirsten Skov for their support and guidance throughout this work and for their advice during the preparation of the thesis. I would also like to thank past and present members of this research group for their help and advice, in particular Chris Alexander, Ken MacFarlane and Richard Schutte. I would like to give a huge thanks to Guy Clentsmith (and also past and present members of Dork International), Murugesapillai Mylvaganam, Pete Caravan (for the English music), and Christian Brückner for their advice and top tips in the caper.

The cheerful group at B. C. Cancer Research Centre especially, Dr. Brian Marples, Hans Adomat, Jadranka Sangulin and Jeff Matthews (for his assistance with the AA machine) are also to be thanked for their assistance with the biological tests.

Chapter 1: Introduction

1.1 Preamble

Cancer is a disease in which cells grow in an uncontrolled way¹ and arises as a result of changes in cellular DNA. These changes can be caused by many factors: environmental factors including ionizing/UV radiation and exposure to carcinogens; an inherited deficiency in ability to repair lesions in DNA; chromosomal changes; the existence of a number of genes ("oncogenes") that can transform normal cells into cancer cells; and the loss or inactivation of "tumour suppressor genes".² To date, 10 tumour suppressor genes have been discovered,³ and of these p53 ('p' for protein and '53' refers to its molecular weight in kilodaltons) has been studied most extensively. It is present in all normal cells and has been found in both inherited and spontaneously occurring cancer. The normal function of p53 is to act as a transcription factor by binding to, and controlling the expression of genes that are involved with cell growth and division.⁴ If DNA is damaged or is incorrectly synthesized, p53 is thought to accumulate and switch off replication to allow time for the DNA to be repaired. If the repair is unsuccessful p53 may also trigger cell suicide by a mechanism known as apoptosis. Cells which contain an inactive p53 gene or non-functional p53 protein cannot carry out this arrest. Consequently, in these cells, a number of different genetic alterations can accumulate, and this may lead to the development of a tumour.⁵

The identification of genetic changes in malignant cells, and the role played in cancer causation by the protein products of involved genes, are central themes of current cancer research.⁶ Of equal importance is the development of chemical compounds that can aid in the diagnosis and treatment of cancer. In this work, several water-soluble ruthenium porphyrin complexes have been synthesized, characterized and evaluated as potential anti-cancer compounds.

1.2 Cancer Treatment

The absence of universal identifiable factors between normal and malignant cells is a serious obstacle that has limited the development of a generally applicable anti-cancer therapy. There are three primary ways to treat cancer: (1) surgery; (2) radiotherapy; and (3) chemotherapy. The second and third categories are areas in which chemists can make a significant contribution.⁷

If a cancer is diagnosed before metastasis has occurred, it is often curable by local treatment, with surgery and/or radiotherapy. If metastasis has occurred then chemotherapy treatment is required using cytotoxic drugs.

1.2.1 Surgery

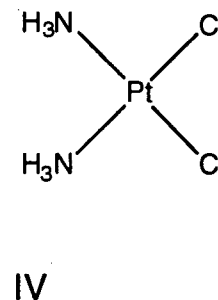
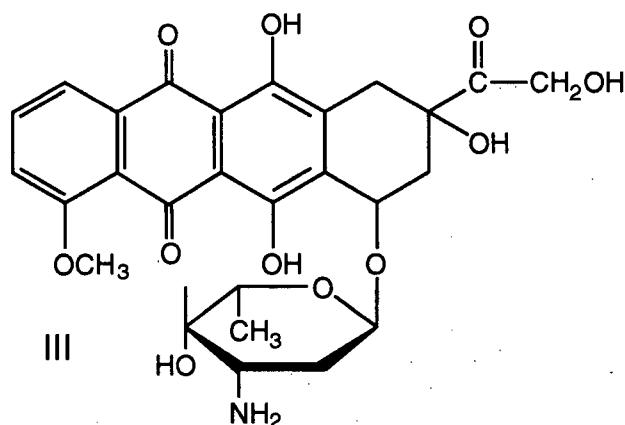
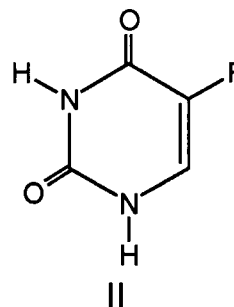
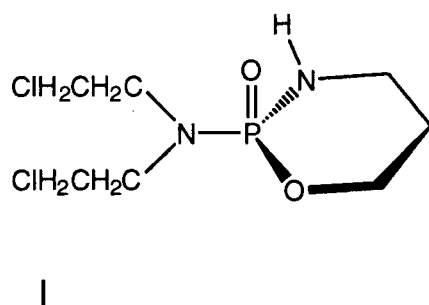
Surgery involves the removal of the tumour with an adequate margin of normal tissue to allow for local invasive spread.⁶

1.2.2 Radiotherapy

Radiotherapy involves the use of many different types of radiation, of which X-rays are the most commonly used. Conventionally, treatment with X-rays involves the administration of 25-35 X-ray dose fractions (~2Gy), spread over a period of 5-7 weeks.⁸ Ionizing radiation is generally believed to cause damage to cells and tissues by depositing energy as a series of discrete events.⁹ This is a random process and thus can cause damage to any molecule in the cell, but the damage to DNA is regarded as the most crucial in relation to cell killing.¹⁰⁻¹² Radiation treatment of tumours inside the body requires that the radiation pass through normal tissue. The main objective of this treatment is therefore to maximize the killing of the tumour cells whilst minimizing the damage to the surrounding normal tissue.⁶ The details of this form of therapy will be dealt with in a later section.

1.2.3 Chemotherapy

Tumours are believed to contain a population of cells known as stem cells. These have a high potential for cell proliferation and are the target of anti-cancer drugs. The mechanism of action of drug therapy generally addresses any process involved in cell division/proliferation, usually DNA replication. The treatment also kills the populations of normal cells in the body which are dividing and therefore produces undesirable side-effects, i.e. nausea, vomiting and hair-loss.^{13,14} In 1942, the first chemotherapy drug (nitrogen mustard) was used to treat cancer. Today there are 35 cytotoxic drugs used in the treatment of patients in North America. These drugs can be loosely classed into four groups: alkylating agents (e.g. **I**, cyclophosphamide); antimetabolites (e.g. **II**, 5-Fluoracil); naturally occurring species (e.g. **III**, Doxorubicin) and miscellaneous compounds (e.g. **IV**, Cis-diamminedichloroplatinum (II) (*Cis-platin*)).¹⁵ Anticancer drugs are used frequently in combination with each other and also with radiation.¹⁶



The major limitation to this form of treatment is the presence in tumours of drug-resistant cells that either produce an initial resistance to treatment or subsequent resistance after the tumour has responded.¹⁷

Alternative approaches are being developed which include Photodynamic Therapy,^{18,19} and Immunotherapy.²⁰

1.3 Effects of Radiation

1.3.1 Radiation-induced DNA damage

Radiation can cause damage to DNA by both direct and indirect actions (see Fig. 1.1).

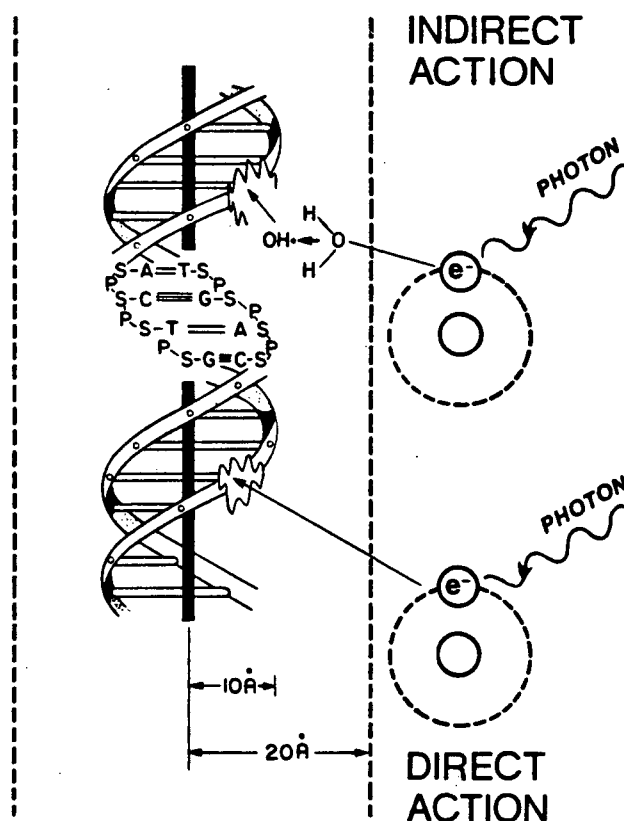
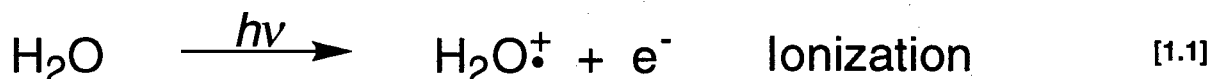


Figure 1.1: Diagram (from Hall²¹) illustrating direct and indirect action of radiation. The structure of DNA is shown schematically; the letters S, P, A, T, G, and C represent sugar, phosphate, adenine, thymine, guanine, and cytosine, respectively.

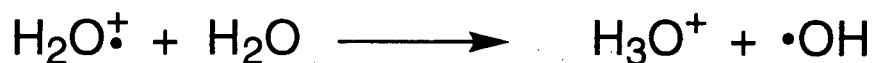
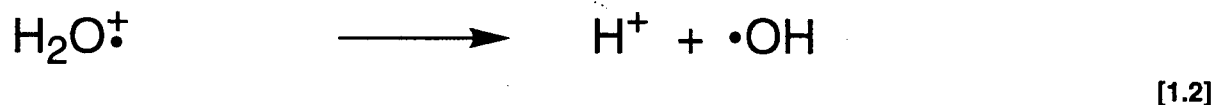
Direct damage is a result of energy being deposited directly into the target molecule DNA. The excited and ionized DNA molecules are unstable and the excess energy is dissipated either by the emission of photons or induces the breakage of a covalent bond within the molecule.²² Two-thirds of the damage to DNA in aerobic cells is a result of the indirect effect.²³ This effect assumes that the damage to DNA does not arise from energy deposited directly in the molecule itself but is caused by the radicals produced by the radiolysis of nearby water molecules.²²

1.3.2 Radiolysis of water

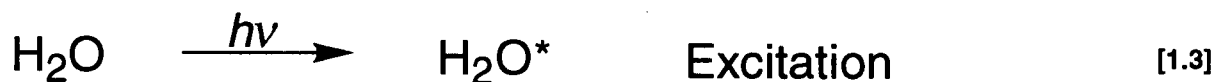
The radiolysis of water involves both the ionization and excitation of the molecules as shown in eqs 1.1-1.4.^{24,25}



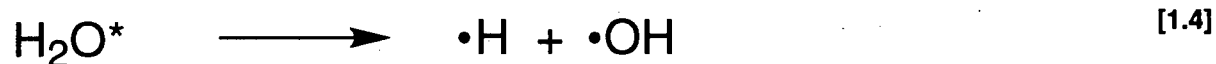
Ionization of water molecules produces an unstable water ion radical and an electron that becomes hydrated ($\text{e}_{(\text{aq})}^-$) within about 10^{-11} s (eq 1.1). The water ion radical then decomposes losing a proton (eq 1.2).



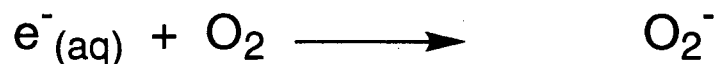
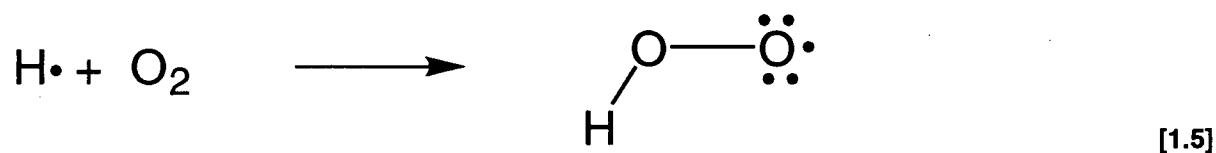
The net result is the formation of protons, hydroxyl radicals and hydrated electrons.



The excited water molecules (eq 1.3) can give free radicals directly, but this mechanism is believed not to contribute significantly to their overall yield because it has too high a kinetic barrier (eq 1.4).



The hydroxyl radical ($\cdot\text{OH}$), a potent oxidizing agent, is believed to be the species most damaging to DNA as it interacts directly with the DNA backbone by electron transfer, or by abstraction of hydrogen or by addition to produce damaging lesions. The hydrogen atom and the hydrated electron are strong reducing agents; in general, reactions with $e_{(\text{aq})}^-$ can result in electron capture or lead to dissociation, while reactions of $\text{H}\cdot$ can lead to additions and abstractions.²⁴ However, in biological systems it is more probable that they will react with dissolved oxygen, which is an effective scavenger of these radicals, to form the peroxide radical and the superoxide anion, respectively (eq 1.5).²⁵



The former is reduced by the enzyme catalase to water and oxygen²⁶ and the latter is rapidly reduced to hydrogen peroxide by the enzyme superoxide dismutase. This idea has been challenged and there is some dispute as to the eventual fate of the superoxide anion.²⁷

1.3.3 Damage fixation[†] by oxygen

Oxygen also 'fixes' the damaged DNA by a mechanism that is in direct competition with the repair processes in which thiols play an important role.^{28,29} There are two possible ways in which oxygen can 'fix' the damage. Firstly, oxygen can react with a radical produced by the radiolysis of water, the radical then reacting irreversibly with DNA to form an organic peroxide (eq 1.6). This can then cause a lethal lesion on DNA thereby making the damage permanent.³⁰



Secondly, an electron excited in DNA by direct interaction with radiation can migrate to electron affinic areas (such as O₂ or another radiosensitizer (discussed in Section 1.4)), thus separating the two charges. If the damaged DNA is not quickly reduced, then it may be further oxidized by oxygen and thus result in fixation of the damage. This reduction process is performed by thiols, via a poorly understood mechanism. Thiols are believed to repair the damage caused by the reactive species formed from the radiolysis of water either by H[•] donation, or by inducing recombination of radicals.³¹

1.3.4 The oxygen effect

The oxygen effect was first discovered as early as 1912 (refer to Section 1.3.3). In the presence of molecular oxygen, cells are much more sensitive to X-rays. This difference in sensitivity can be partially attributed to the contributions that indirect damage plays in cell killing. The ratio of doses needed to produce the same level of cell killing under oxic (presence of oxygen) and hypoxic (lower oxygen content) conditions is called the oxygen

[†] to make permanent or irreparable

enhancement ratio (OER). The dose response curve (Fig. 1.2) shows that hypoxic cells typically require three times the dose of the oxygenated cells to achieve the same surviving fraction.³²

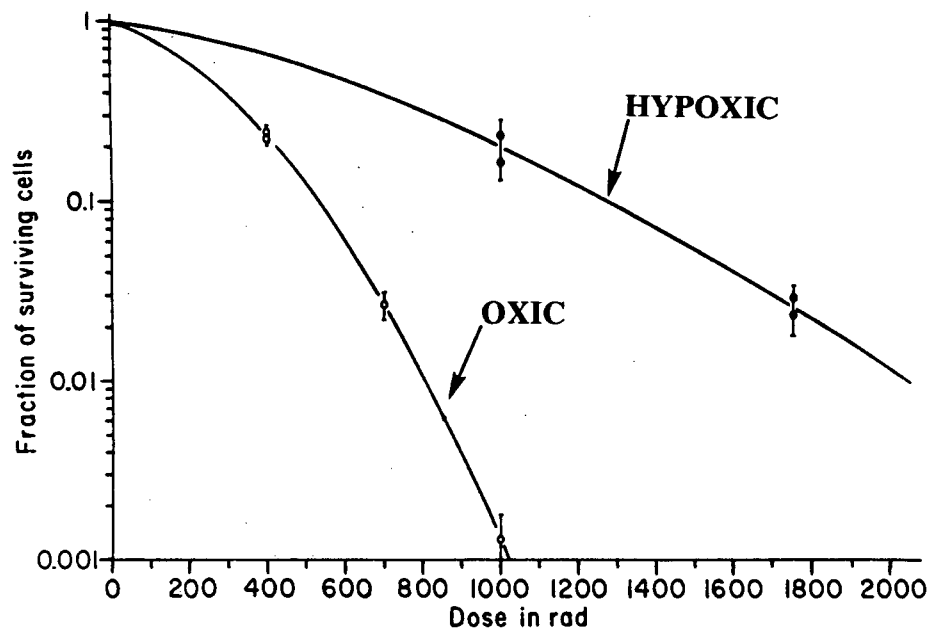


Figure 1.2: A typical survival curve for Chinese Hamster Ovary (CHO) cells as a function of radiation dose.³²

1.3.5 Hypoxia

One of the main problems which limits the success of radiotherapy is the presence of hypoxic cells in tumours. Hypoxic tissue occurs 150-200 μm away from the blood capillaries in a tumour, the effective diffusion distance of oxygen³³, and develops as a result of the imbalance between tumour cell production and the expansion of the vascular network.³⁴ The lower oxygen content of the hypoxic cells as compared to the surrounding tissue leads to increased radioresistance.

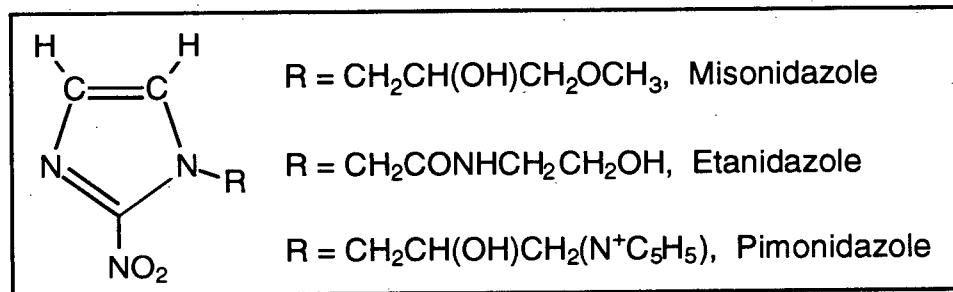
The presence of radioresistant hypoxic cells creates a considerable problem if tumours are to be treated with large doses of radiation, because these cells are capable of being reoxygenated post irradiation; this is one rationale for fractionated treatment. Consequently, small doses are given in a series of repeated fractions and so tumour regrowth is inhibited.³⁴

Several other approaches have been adopted to improve the "dose-delivery" to the tumour. High energy radiations (pions) have been employed which cause proportionally more damage in the tumour site than the normal tissue compared to X-rays, which has proved to be more successful with deep-seated tumours.³⁵ An alternative approach is to biochemically/chemically modify the effectiveness of X-rays, which has been achieved by exploiting biological differences between normal tissues and tumour cells. The use of radiosensitizers is a good example of this type of approach.

1.4 Radiosensitizers

Radiosensitizers increase the sensitivity of hypoxic cells to radiation by mimicking the radiosensitizing properties of oxygen, the most important of which is its so-called electron affinity.³⁶ Oxygen and electron-affinic agents increase the radiation sensitivity of hypoxic cells by fast free-radical mechanisms.³⁷

Since 1973, a series of potentially therapeutic compounds known as the nitroimidazoles (examples shown below) have been studied.



In the laboratory, misonidazole has been the most extensively studied nitroimidazole.^{36,38} It sensitizes hypoxic cells but not oxygenated cells although the potential benefits of this compound are severely limited by its neurotoxicity. Many second generation compounds have been synthesized, e.g. Etanidazole (SR 2508) and Pimonidazole (Ro 03-8799).³⁹ Etanidazole has reduced lipophilicity and hence is less neurotoxic.⁴⁰ It can therefore be administered at higher concentrations than misonidazole and sensitizes the hypoxic cells more effectively.⁴¹ Etanidazole is still undergoing clinical trials.

1.5 Radiosensitizer Drug Design

The effectiveness of most of the anticancer compounds used today is due to the various ways in which they interact with DNA.⁴² It is also believed that DNA is the crucial target for radiosensitizers. Ideally, the design of such compounds requires that they should preferentially accumulate at the site of a tumour, have the ability to target DNA, and contain some functionality that can mimic the electron affinity of oxygen.

1.5.1 Tumour accumulation and localization

The properties listed above could be achieved by using a compound such as a porphyrin. There is widespread belief that porphyrins preferentially accumulate in tumour cells as compared to the surrounding tissue,⁴³⁻⁴⁶ although *in vivo* results have been

equivocal.⁴⁷⁻⁴⁹ Porphyrins have been shown to localize in various sites of a tumour cell; e.g. the anionic, free-base porphyrin, $H_2(TSPP)^{4-}$, has been shown to locate in the tumour stroma,⁵⁰ whereas the cationic, free-base porphyrin, $H_2(TMPyP)^{4+}$, is transported to the mitochondria.⁵¹ The route by which the porphyrin is transported to the tumour *in vivo* may vary depending on the porphyrin.⁵²⁻⁵⁵

Porphyrins have the potential to be used as radiosensitizers *in vivo* because they have been shown to bind to DNA,⁵⁶⁻⁶¹ to be non-toxic to normal cells,^{62,63} and to localize and accumulate in tumour cells.^{43-46,50,51} Certain free-base, and cobalt and copper porphyrins have also exhibited some radiosensitizing properties.^{62,64}

Porphyrin compounds have also been studied in clinical chemistry related to porphyria, as anti-cancer drugs for boron neutron capture therapy,^{46,65} photodynamic therapy,¹⁹ as contrast agents in nuclear magnetic resonance imaging (MRI),^{66,67} and in AIDS research.⁶⁸

1.5.2 DNA binders

Some transition metals can target the DNA of a tumour cell. This has been shown with the chemotherapy drug *Cis-platin*. The 1,2-intra-strand cross-link lesion formed when *Cis-platin* binds to DNA is believed to be the crucial factor responsible for the antitumour effect.⁶⁹ Following the successful clinical application of *Cis-platin*, a number of complexes containing ruthenium have been evaluated with regard to their anticancer potential⁷⁰⁻⁸⁰ with the aim of developing a metal based complex that would be less toxic than *Cis-platin*.

Initial studies of ruthenium complexes with NH_3 and Cl^- as ligands showed good activities in the treatment of tumours *in vivo*; ⁷³ *trans*- $RuCl_4(imidazole)_2^-$ is a particularly attractive candidate.⁷⁷ Also, ruthenium(II) dimethylsulfoxide complexes have been shown to possess significant antitumour activity, comparable to that of *Cis-platin* and with much less toxic side-effects.⁷¹

Ruthenium in the essentially octahedral complex, *trans*-RuCl₂(DMSO)₄ has been shown to bind in the same way as *Cis*-platin to the N7 atoms of two guanine molecules of DNA *in vitro*,^{79,80} which indicates that the interaction with DNA is not exclusive to platinum or to metals with a cis, square planar geometry.

1.5.3 Metalloporphyrin complexes

Previous work in this laboratory has established that water-soluble Pt porphyrins have low toxicity, exhibit high accumulation in cells, but possess no significant radiosensitizing properties.⁶³ The combination of a ligand such as a porphyrin that can accumulate at a tumour, and a metal such as ruthenium, that can bind to DNA, presents a rational approach to the design of an inorganic complex as a radiosensitizer and as an antitumour compound. It seemed logical to extend this work to the ruthenium nucleus, which in various complexes (*vide supra*), possesses some interesting anticancer properties.

1.6 The Scope of the Thesis

In this work, the synthesis and characterization of several water-soluble, ruthenium porphyrin complexes were carried out, and their potential as radiosensitizer compounds was explored. Chapter 2 describes the experimental procedures used. Chapter 3 discusses the chemistry involved in the synthesis of the metalloporphyrins. Chapter 4 describes the biological activity of the Ru porphyrin complexes synthesized here and evaluates their *in vitro* potential. Only one report has thus far appeared in the literature on the direct formation of a water-soluble ruthenium porphyrin complex; this involved the metallation of the anionic, free-base porphyrin, H₂(TSPP)⁴⁻ with Ru₃(CO)₁₂.⁸¹ The crux of this thesis was the observation that the easily accessed Ru(III) precursor, [Ru(DMF)₆](CF₃SO₃)₃, can undergo facile reduction in the presence of H₂(TSPP)⁴⁻ to generate a Ru(II) species containing a water-soluble porphyrin ligand. The biological application of this work, while necessarily

unrealized, shows interesting *in vitro* results with respect to the DNA binding and radiosensitization experiments.

1.7 References

- (1) Oppenheimer, S. B. *Cancer, A Biological and Clinical Introduction*; 2nd ed.; Jones and Bartlett Publishers, Inc.: Boston, 1985, p 5.
- (2) Tannock, I. F.; Hill, R. P. In *The Basic Science of Oncology*; 2nd ed.; I. F. Tannock and R. P. Hill, Ed.; McGraw-Hill, Inc.: New York, 1992; p 2.
- (3) Marx, J. *Science* **1993**, 261, 1385.
- (4) Culotta, E. C.; Koshland, D. E. *Science* **1993**, 262, 1958.
- (5) Lane, D. P. *News and Views* **1992**, 358, 15.
- (6) See reference 2, p 3.
- (7) Silverman, R. B. *The Organic Chemistry of Drug Design and Drug Action*; Academic Press, Inc.: San Diego, 1992, p 202-207, 242-254.
- (8) Hill, R. P. In *The Basic Science of Oncology*; I. F. Tannock and R. P. Hill, Ed.; McGraw-Hill, Inc.: New York, 1992; p 298.
- (9) See reference 8, p 273.
- (10) Adams, G. E. In *The Biological Basis of Radiotherapy*; 2nd ed.; G. G. Steel, G. E. Adams and A. Horwich, Ed.; Elsevier: Amsterdam, 1989; p 6.
- (11) Hall, E. J. *Radiobiology for the Radiobiologist*; 3rd ed.; J. B. Lippincott: London, 1988, p 10.
- (12) See reference 8, p 274.
- (13) Roberts, L. *Cancer Today; Origins, Prevention and Treatment*; National Academy Press: Washington D C, 1984, p 11.
- (14) Erlichman, C. In *The Basic Science of Oncology*; I. F. Tannock and R. P. Hill, Ed.; McGraw-Hill, Inc.: New York, 1992; p 334.
- (15) Tannock, I. F. In *The Basic Science of Oncology*; 2nd ed.; I. F. Tannock and R. P. Hill, Ed.; McGraw-Hill, Inc.: New York, 1992; p 302-303.

- (16) See reference 15, p 357.
- (17) See reference 2, p 4.
- (18) See reference 8, p 371.
- (19) Dolphin, D. *Can. J. Chem.* **1994**, 72, 1005.
- (20) Miller, R. G.; Tannock, I. F. In *The Basic Science of Oncology*; I. F. Tannock and R. P. Hill, Ed.; McGraw-Hill, Inc.: New York, 1992; p 252.
- (21) See reference 11, p 11.
- (22) Tubiana, M.; Dutreix, J.; Wambersie, A. *Introduction to Radiobiology*; Taylor & Francis: London, 1990, p 26-27.
- (23) See reference 11, p 15.
- (24) Bielski, B. H. J.; Gebicki, J. M. *Free Radicals in Biology*; Academic Press: New York, 1977; Vol. III, p 18-23.
- (25) See reference 22, p 23-25.
- (26) Stryer, L. *Biochemistry*; 3rd ed.; W. H. Freeman & Company: New York, 1988, p 422.
- (27) Sonntag, C. V. *The Chemical Basis of Radiation Biology*; Taylor & Francis: London, 1987, p 57-59.
- (28) Denekamp, J. In *The Biological Basis of Radiotherapy*; 2nd ed.; G. G. Steel, G. E. Adams and A. Horwich, Ed.; Elsevier: Amsterdam, 1989; p 123.
- (29) Ward, J. F. *Radioprotectors and Anticarcinogens*; Academic Press: 1983, p 73.
- (30) See reference 11, p 141.
- (31) See reference 22, p 31-32.
- (32) See reference 11, p 138-140.
- (33) See reference 11, p 158.
- (34) See reference 27, p 131.
- (35) See reference 8, p 276.
- (36) See reference 8, p 292.

- (37) See reference 11, p 198.
- (38) Stratford, I. J.; Adams, G. E. In *The Biological Basis of Radiotherapy*; 2nd ed.; G. G. Steel, G. E. Adams and A. Horwich, Ed.; Elsevier: Amsterdam, 1989; p 145.
- (39) See reference 11, p 184.
- (40) See reference 38, p 151.
- (41) See reference 8, p 293.
- (42) See reference 7, p 235-271.
- (43) Woodburn, K. W.; Stylli, S.; Hill, J. S.; Kaye, A. H.; Reiss, J. A.; Phillips, D. R. *Br. J. Cancer* **1992**, *65*, 321.
- (44) Winkelman, J. W. *Methods in Porphyrin Photosensitization*; Plenum Press: New York, 1985; Vol. 193, p 91.
- (45) Nakajima, S.; Hayashi, H.; Omote, Y.; Yamazaki, Y.; Hirata, S.; Maeda, T.; Kubo, Y.; Takemura, T.; Kakiuchi, Y.; Shindo, Y. *Photochem. Photobiol.* **1990**, *7*, 189.
- (46) Hill, J. S.; Kahl, S. B.; Kaye, A. H.; Stylli, S. S.; Koo, M. S.; Gonzales, M. F.; Vardaxis, N. J.; Johnson, C. I. *Proc. Natl. Acad. Sci. USA* **1992**, *89*, 1785.
- (47) Reddi, E.; Segalla, A.; Jori, G.; Kerrigan, P. K.; Liddell, P. A.; Moore, A. L.; Moore, T. A.; Gust, D. *Br. J. Cancer* **1994**, *69*, 40.
- (48) Quastel, M. R.; Richter, A. M.; Levy, J. G. *Br. J. Cancer* **1990**, *62*, 885.
- (49) Gomer, C. J.; Dougherty, T. J. *Cancer Res.* **1979**, *39*, 146.
- (50) Kessel, D.; Thompson, P.; Saatio, K.; Nantwi, K. D. *Photochem. Photobiol.* **1987**, *45*, 787.
- (51) Woodburn, K.; Vardaxis, N. J.; Hill, J. S.; Kaye, A. H.; Reiss, J. A.; Phillips, D. R. *Photochem. Photobiol.* **1992**, *55*, 697.
- (52) Villanueva, A.; Jori, G. *Cancer Letters* **1993**, *73*, 59.
- (53) Maziere, J. C.; Morliere, P.; Santus, R. *Photochem. Photobiol.* **1991**, *8*, 351.
- (54) Stout, D. L. *Biochem. Biophys. Res. Commun.* **1992**, *189*, 765.

- (55) Hamori, C. J.; Lasic, D. D.; Vreman, H. J.; Stevenson, D. K. *Pediatric Res.* **1993**, 34, 1.
- (56) Kuroda, R.; Takahashi, E.; Austin, C. A.; Fisher, L. M. *FEBS Letters* **1990**, 262, 293.
- (57) Greiner, S. P.; Kreilick, R. W.; Marzilli, L. G. *J. Biomol. Struct. & Dynamics* **1992**, 9, 837.
- (58) Gray, T. A.; Yue, K. T.; Marzilli, L. G. *J. Inorg. Biochem.* **1991**, 41, 205.
- (59) Strickland, J. A.; Marzilli, L. G.; Gay, K. M.; Wilson, W. D. *Biochemistry* **1988**, 27, 8870.
- (60) Pasternack, R. F.; Gibbs, E. J.; Villafranca, J. J. *Biochemistry* **1983**, 22, 2406.
- (61) Pasternack, R. F.; Gibbs, E. J. *Metal-DNA Chemistry*; A. C. S. Symp. Series: Washington D. C., 1989, p 59.
- (62) Meng, G. G. Ph D Thesis, University of British Columbia, 1993.
- (63) Ravensbergen, J. A. M. Sc. Thesis, University of British Columbia, 1993.
- (64) O'Hara, J. A.; Duple, E. B.; Abrams, M. J.; Picker, D. J.; Giandomenico, C. M.; Vollano, J. F. *Int. J. Radiat. Oncol. Biol. Phys.* **1989**, 16, 1049.
- (65) Nguyen, T.; Brownell, G. L.; Holden, S. A.; Kahl, S.; Miura, M.; Teicher, B. A. *Radiat. Res.* **1993**, 133, 33.
- (66) Zijl, P. C. v.; Place, D. A.; Cohen, J. S.; Fuastino, P. J.; Lyon, R. C.; Patronas, N. J. *Acta Radiologica* **1990**, 374, 75.
- (67) Hindre, F.; Le Plouzenec, M.; de Certaines, J. D.; Foulter, M. T.; Patrice, T.; Simonneaux, G. *Magn. Reson. Imaging* **1993**, 3, 59.
- (68) Meurier, B. *Chem. Rev.* **1994**, 92, 1411.
- (69) Sherman, S. E.; Lippard, S. J. *Chem. Rev.* **1987**, 87, 1153.
- (70) Sava, G.; Pacor, S.; Zorzet, S.; Alessio, E.; Mestroni, G. *Pharmacol. Res.* **1989**, 21, 617.
- (71) Sava, G.; Zorzet, S.; Giraldi, T.; Mestroni, G.; Zassinovich, G. *Eur. J. Cancer Clin. Oncol.* **1984**, 20, 841.

- (72) Chan, P. K.; Chan, P. K. H.; Frost, D. C.; James, B. R.; Skov, K. A. *Can. J. Chem.* **1988**, *66*, 117.
- (73) Clarke, M. J. *Metal Ions in Biological Systems*; Marcel Dekker, Inc.: New York, 1980; Vol. 11, p 231.
- (74) Hammershoi, A.; Nord, G.; Rowatt, E.; Skov, L. K.; Williams, R. J. *J. Inorg. Biochem.* **1993**, *49*, 295.
- (75) Bregant, F.; Pacor, S.; Ghosh, S.; Chattopadyay, S. K.; Sava, G. *Anticancer Res.* **1993**, *13*, 1101.
- (76) Fruhauf, S.; Zeller, W. J. *Cancer Chemotherapy & Pharmacology* **1991**, *27*, 301.
- (77) Kratz, F.; Hartmann, M.; Keppler, B.; Messori, L. *J. Biol. Chem.* **1994**, *269*, 2581.
- (78) Sava, G.; Pacor, S.; Mestroni, G.; Alessio, E. *Clin. Exp. Metastasis* **1992**, *10*, 273.
- (79) Cauci, S.; Viglino, P.; Esposito, G.; Quadrifoglio, F. *J. Inorg. Biochem.* **1991**, *43*, 739.
- (80) Esposito, G.; Cauci, S.; Fogolari, F.; Alessio, E.; Scocchi, M.; Quadrifoglio, F.; Viglino, P. *Biochemistry* **1992**, *31*, 7094.
- (81) Pawlik, M.; Hoq, M. F.; Shepherd, R. E. *J. Chem. Soc., Chem. Commun.* **1983**, 1467.

Chapter 2: Experimental Section for the Synthetic Inorganic and Organic Chemistry

2.1 Reagents

Pyrrole and 4-pyridinecarboxaldehyde were purchased from Aldrich. The pyrrole was vacuum distilled prior to use, whilst the aldehyde was used as supplied. Ruthenium was supplied by Johnson Matthey Ltd. as $\text{RuCl}_3 \cdot x\text{H}_2\text{O}^\dagger$ (41.91% Ru). $\text{LiN}(\text{SiMe}_3)_2$ was kindly donated by Prof. Michael Fryzuk's group in this department. Hexanes were dried over sodium benzophenone ketyl under argon, and DMF was dried over 4 Å molecular sieves. All other chemicals and solvents were reagent grade or purer and the solvents were used without drying, except where mentioned. Water was distilled and deionised before use. ^{13}CO was purchased from Cambridge Isotope Laboratories. Silica gel (grade 60, 230-400 mesh) was purchased from BDH, and alumina (neutral, Brockman activity I) was purchased from Fisher chemicals. Celite 545 was supplied by Fisher Chemicals and granular Sn (30 mesh) was supplied by Mallinckrodt. Molecular porous membrane tubing (molecular weight cut off = 1,000 g mol⁻¹) was purchased from Spectra/Por.

2.2 Physical Techniques and Methods

^1H NMR spectra were recorded at room temperature, except where mentioned, on Varian XL-300 or Bruker AMX-500 instruments operating at 300.12 and 500.13 MHz respectively; the high pressure ^1H NMR experiment was carried out in a sapphire NMR tube (see Section 3.4). $^{13}\text{C}\{^1\text{H}\}$ NMR spectra were recorded at room temperature on the Varian instrument operating at 75.1 MHz. ^1H NMR spectra were referenced to internal $\text{D}_3\text{CSOCD}_2\text{H}$ (present in d_6 -DMSO) at 2.49 ppm, and $^{13}\text{C}\{^1\text{H}\}$ NMR spectra to internal D_3CSOCD_3 at 39.5 ppm with respect to TMS at 0.0 ppm. d_6 -DMSO was distilled from CaH_2 and was degassed by three freeze-pump-thaw cycles. Infrared spectra were recorded

[†] The samples approximate to a trihydrate composition.

on an ATI Mattson Genesis Series FTIR spectrophotometer as KBr discs or as solutions between NaCl discs, and UV/visible spectra were recorded at room temperature, except where mentioned, on a Hewlett Packard 8452A Diode Array spectrophotometer with 0.1 cm and 1 cm quartz cells. UV/visible data for the free base porphyrins and the metalloporphyrins are reported in Table 2.1. Elemental analyses (C, H, N) were performed by P. Borda of this department. Dialysis was performed by the use of a molecular porous membrane. Typically a length of tubing (10 cm long) was charged with an aqueous solution of the metalloporphyrin. The tubing was closed with clips and immersed in a large volume of distilled water (2 L). After 2 hours of being stirred, the water was replaced by a fresh volume and stirring was continued for a further 2 hours. After dialysis, the solution inside the tubing was evaporated to dryness on a rotary evaporator. Photolysis was performed by means of a 450 Watt Hanovia mercury vapour lamp (Fisher Co.), as described by earlier work from this laboratory.¹

2.3 Syntheses of the Free-Base Porphyrins

2.3.1 Syntheses of H₂(TPP), H₂(TPyP) and H₂(TMPyP)⁴⁺†

The porphyrins H₂(TPP)², H₂(TPyP)² and H₂(TMPyP)⁴⁺ 2,3 were prepared exactly according to the literature procedures. H₂(TPP) and H₂(TMPyP)⁴⁺ were kindly donated by G. Meng and by J. Ravensbergen, respectively. In some of the preparations, the crude H₂(TPP) was purified by column chromatography on silica gel using CHCl₃ as the eluent.^{4b} The UV/visible data for the free base porphyrins are given in Table 2.1 (page 27). The NMR data for H₂(TPP), H₂(TPyP) and H₂(TMPyP)⁴⁺ agree well with those in the literature.^{4b,5} The elemental analysis for H₂(TPyP) (Found (calcd) : C, 76.76 (77.65); H 4.63, (4.24); N 16.60 (18.11)) indicated that the compound was not quite pure; further purification was not

† For convenience, this tetratosylate salt is sometimes written as H₂(TMPyP)⁴⁺.

attempted because the porphyrin was to be used in several NMR scale reactions (see Sections 2.5.2 and 3.5) in which analytical purity was considered not to be vital.

2.3.2 Synthesis of $\text{Na}_4[\text{H}_2(\text{TSPP})]^\dagger$

The synthesis of $\text{Na}_4[\text{H}_2(\text{TSPP})]$ was based on a literature procedure⁶ which had been modified and described earlier.^{4a,7} $\text{H}_2(\text{TPP})$ (0.500 g, 0.819 mmol) was mixed with concentrated sulfuric acid (10 mL) to give a green slurry. The reaction mixture was heated in an oil-bath at 100-110 °C for 12 hours. After the reaction mixture had cooled to room temperature, ice-cold water (50 mL) was added slowly. The mixture was cooled by an ice-bath and was carefully neutralized with concentrated NaOH and dilute Na_2CO_3 to pH = 8-9. Upon neutralization the green solution turned to a dark purple solution. The solution was concentrated by evacuation at room temperature (20 mL) and cooled in an ice-bath (the precipitate that formed was mainly Na_2SO_4). Methanol (250 mL) was added to the mixture and this was then filtered through a layer of Celite to remove the salts. The filtration was repeated and the solvent of the filtrate was removed to give a dark purple residue which was redissolved in methanol (100 mL). The remaining dark residue (mainly inorganic salts with adsorbed porphyrin) that remained was dissolved in a minimum amount of hot water, reprecipitated with methanol (50 mL) and then filtered. The methanol solutions were combined and evaporated to dryness on a rotary evaporator, and the purple residue was collected, and dried under vacuum at 100 °C overnight to give the crude product.

The crude product was dissolved in methanol (45 mL), and the solution was filtered. (If a dark residue remained, this was dissolved in a minimum of hot water, reprecipitated with methanol (50 mL) and then filtered.) To the filtrate, acetone (200 mL, dried over 4Å sieves) was added with stirring; a purple precipitate formed which was filtered off and air-dried. This methanol-acetone reprecipitation procedure was repeated two more times. The

[†] For convenience, this tetrasodium salt is sometimes written as $\text{H}_2(\text{TSPP})^{4-}$.

purple product was then dissolved in water, the solvent was then removed and the final (less hygroscopic) product was collected and dried at 100 °C *in vacuo* (0.624g, 75% yield). Anal. Calcd for $C_{44}H_{32}N_4Na_4O_{15}S_4$ (i.e. $Na_4[H_2(TSPP)] \cdot 3H_2O$): C, 49.07; H, 2.99; N, 5.20. Found: C, 49.20; H, 2.97; N, 5.18. 1H NMR (d_6 -DMSO, 300 MHz) δ 8.88 (s, 8H, pyrrole-H), 8.17 (d, 8H, *m*- $C_6H_4SO_3^-$), 8.03 (d, 8H, *o*- $C_6H_4SO_3^-$), -2.95 (s, 2H, NH). UV/visible data are given in Table 2.1.

2.4 Preparation of the Ruthenium Precursor Complexes

2.4.1 $Ru_3(CO)_{12}$

Crude $Ru_3(CO)_{12}$ was prepared according to a literature procedure⁸, and was kindly donated by C. Alexander. The complex was purified by passage through a column of alumina with CH_2Cl_2 eluent. The CH_2Cl_2 was removed to leave an orange crystalline material which gave an infrared spectrum that agreed with the literature data.⁸

2.4.2 *Cis*- $RuCl_2(DMSO)_4$

Cis- $RuCl_2(DMSO)_4$ was prepared according to a literature procedure⁹ and was kindly donated by D. Yapp.

2.4.3 $[Ru(DMF)_6](OTf)_3$

The $[Ru(DMF)_6](OTf)_3$ was prepared following a modified literature procedure.¹⁰ A solution of $RuCl_3 \cdot 3H_2O$ (2.00 g, 9.88 mmol) in DMF (120 mL) with Sn granules (7.0 g, 5.90×10^{-2} mol) was vigorously stirred at ambient temperature under nitrogen. The solution turned from dark-brown, through red-brown and green to blue. $Pb(OTf)_2$ (6.50 g, 12.9 mmol) was added to the blue solution. The mixture was stirred at 50 °C for 2 hours, during which time the solution changed to a deep brown-red colour. This was then filtered to remove unreacted Sn and was concentrated on a rotary evaporator to 20 mL (temperature < 65 °C). CH_2Cl_2 (300 mL) was added, and this mixture was then stirred in air at room

temperature overnight. The solution was filtered through a layer of Celite and the PbCl_2 retained by the frit was discarded. Filtration was repeated through Celite until no more salts were collected. CH_2Cl_2 was removed on the rotary evaporator. To the mixture at room temperature was added 1,2- $\text{C}_2\text{H}_4\text{Cl}_2$ (40 mL), after which the solution was cooled to 4 °C to give a yellow precipitate. The precipitate was recovered on a frit, redissolved in CH_2Cl_2 , the mixture was then filtered, and the yellow solution was evaporated to dryness. The yellow precipitate was shaken with n-pentanol (5 mL), recovered on a frit, washed with Et_2O (50 mL), and dried *in vacuo* (1.78 g, 21% yield). Anal. Calcd. for $\text{C}_{21}\text{H}_{42}\text{F}_9\text{N}_6\text{O}_{15}\text{RuS}_3$: C, 25.56; H, 4.29; N, 8.52. Found: C, 25.46; H, 4.34; N, 8.46.

Synthesis of $\text{Pb}(\text{OTf})_2$

$\text{CF}_3\text{SO}_3\text{H}$ (11 mL, 0.124 mol) was added dropwise with stirring to PbCO_3 (5.50 g, 20.6 mmol). The mixture was then left for 20 minutes and Et_2O (80 mL) was added. The white slurry was filtered and the white solid was washed with Et_2O (100 mL) and dried *in vacuo* (8.20g, 80% yield).

2.5 Metallation Reactions

2.5.1 Synthesis of $\text{Na}_4[\text{Ru}(\text{TSPP})(\text{CO})(\text{DMF})]^\dagger$ (1)

Method (a)

To a slurry of $\text{H}_2(\text{TSPP})^{4-}$ (0.200 g, 0.196 mmol) in DMF (130 mL, dried over 4 Å sieves) was added $\text{Ru}_3(\text{CO})_{12}$ (0.125 g, 0.196 mmol). The dark purple solution was refluxed under nitrogen for 2-3 weeks. The resulting dark red solution was filtered through Celite to remove any precipitated metallic Ru. The solvent was then removed on the rotary evaporator and the dark purple residue was dissolved in a minimum amount of water (5 mL) and dialysis was performed to purify the product. The solvent was removed and the purple crystalline

[†] For convenience, the tetrasodium salt is sometimes written as $\text{Ru}(\text{TSPP})(\text{CO})(\text{DMF})^{4-}$.

residue was dried at 100 °C *in vacuo* (0.214 g, 96% yield). Anal. Calcd. for $C_{45}H_{36}N_4Na_4O_{19}RuS_4$ (i.e. $Na_4[Ru(TSPP)(CO)(DMF)] \cdot 6H_2O$): C, 42.96; H, 2.88; N, 4.45. Found C, 42.81; H, 2.58; N, 4.98. 1H NMR (d_6 -DMSO, 300 MHz) δ 8.55 (s, 8H, pyrrole-H), 8.13 (m, 8H, *m*- $C_6H_4SO_3^-$), 8.01 (m, 8H, *o*- $C_6H_4SO_3^-$), -2.30 (s, 1H, bound-C(O)NH), -3.17 and -3.19 (s, 3H, bound-N(CH_3)(CH'_3)), (see Section 3.3.1). IR (KBr disc) ν_{CO} 2027, 1971, 1929 cm^{-1} . UV/visible data are given in Table 2.1.

Method (b)

The solution reaction had to be carried out in the dark because the ruthenium starting material is light-sensitive. A slurry of $H_2(TSPP)^{4-}$ (0.210 g, 0.205 mmol) in DMF (80 mL) was heated to 50 °C and a bright yellow solution of $[Ru(DMF)_6](OTf)_3$ (0.614 g, 0.622 mmol) in DMF (20 mL) was added. The resulting dark purple solution was then heated to reflux under an atmosphere of nitrogen for 3 hours. The resulting dark red solution was filtered through Celite to remove any Ru metal that was present and the filtrate was concentrated to 10 mL by evaporation. Acetone (10 mL) was added and a dark red precipitate formed immediately. The mixture was then filtered through a medium frit to give a cloudy red filtrate and a dark purple solid that was retained by the frit. The filtrate was concentrated to dryness. The resulting dark red residue was redissolved in DMF (5 mL) and the product was precipitated using CH_2Cl_2 (5 mL). The crude products were then combined and dried *in vacuo* at 100 °C. The purple compound was redissolved in a minimum of hot DMF (5-10 mL) and then was filtered through a layer of Celite, to remove any insoluble impurities. The product was precipitated with two volumes of CH_2Cl_2 (5-10 mL) and collected on a frit. The purple products were then combined and dried overnight at 100 °C *in vacuo* (0.059 g, 25% yield). Isolated crystals were submitted for X-ray crystallographic analysis but were found to be twinned. Anal. Calcd for $C_{54}H_{49}N_7Na_4O_{18}RuS_4$ (i.e. $Na_4[Ru(TSPP)(CO)(DMF)] \cdot 2DMF \cdot 2H_2O$): C, 46.15; H, 3.51; N, 6.98. Found: C, 46.11; H, 3.75; N, 7.33. 1H NMR (d_6 -DMSO, 300 MHz) δ 8.55 (s, 8H, pyrrole-H), 8.13 (m, 8H, *m*-

$\text{C}_6\text{H}_4\text{SO}_3^-$), 8.01 (m, 8H, $o\text{-C}_6\text{H}_4\text{SO}_3^-$), -2.30 (s, 1H, bound-C(O)NH), -3.17 and -3.19 (s, 3H, bound-N(CH₃)(CH'₃), 7.99 (s, 2H, free-C(O)NH), 2.90 and 2.70 (s, 3H, free-N(CH₃)(CH'₃); ¹H NMR (*d*₆-DMSO, 500 MHz) δ 8.55 (s, 8H, pyrrole-H), 8.14 (d, 4H, $J_{\text{HH}'} = 7.8$ Hz, $m\text{-C}_6\text{H}_4\text{SO}_3^-$), 8.03 (d, 4H, $J_{\text{HH}'} = 7.8$ Hz, $m\text{-C}_6\text{H}_4\text{SO}_3^-$), 7.99 (overlapping dd, 8H, $J_{\text{HH}'} = 7.1$ Hz, $o\text{-C}_6\text{H}_4\text{SO}_3^-$); ¹³C(¹H) (*d*₆-DMSO, 75 MHz) 179.8 (s, CO),* 147.4 (s, C $_{\alpha}$), 143.1 (s, C₁), 142.0 (s, C₄), 133.1 (s, C₂/C₆), 131.6 (s, C _{β}), 123.9 (s, C₃/C₅), 121.2 (s, C_{meso}) (see Section 3.4, Fig. 3.4 and Appendix II). IR (KBr disc) ν_{CO} 2035, 1959, 1924 cm^{-1} (see appendix I); (DMSO) 1913 cm^{-1} . UV/visible data are given in Table 2.1.

2.5.2 Reaction of [Ru(DMF)₆](OTf)₃ with H₂(TPyP)

To a slurry of H₂(TPyP) (0.005 g, 8.08×10^{-6} mol) in DMF (7 mL) was added a bright yellow solution of [Ru(DMF)₆](OTf)₃ (0.027 g, 2.74×10^{-5} mol) in DMF (2 mL). The solution was heated to reflux under an atmosphere of nitrogen for 24 hours. The resulting dark red/brown solution was filtered to remove any precipitated metallic Ru and then evacuated to dryness to give a red product that was insoluble in all common solvents. A UV/visible spectrum was taken of the *in-situ* product (see Table 2.1).

2.5.3 Reaction of [Ru(DMF)₆](OTf)₃ with H₂(TMPyP)⁴⁺

The same method was used as for the previous experiment but using instead H₂(TMPyP)⁴⁺ (0.005 g, 3.67×10^{-6} mol) with [Ru(DMF)₆](OTf)₃ (0.011 g, 1.11×10^{-5} mol) in DMF (10 mL). The cherry red solution was heated to reflux overnight. The resulting dark red/brown solution was filtered to remove any precipitated metallic Ru and a UV/visible spectrum was taken of the *in-situ* product (see Table 2.1). The ¹H NMR spectrum showed the disappearance of the pyrrole N-H peak of the free-base porphyrin (see Section 3.5) but further characterization was not carried out.

* Value measured for a ¹³CO enriched sample (see Section 3.4).

2.5.4 Reaction of $[\text{Ru}(\text{DMF})_6](\text{OTf})_3$ with $\text{H}_2(\text{TPP})$

The same method was used as in Section 2.5.2 but using instead $\text{H}_2(\text{TPP})$ (0.006 g, 1.01×10^{-5} mol) with $[\text{Ru}(\text{DMF})_6](\text{OTf})_3$ (0.030 g, 3.03×10^{-5} mol) in DMF (2.5 mL). The dark purple solution was heated to reflux overnight and a UV/visible spectrum was taken of the *in-situ* product (see Table 2.1).

2.6 Synthesis of $\text{Na}_4[\text{Ru}(\text{TSPP})(\text{DMSO})_2]^\dagger$ (2)

(a) Photolysis

$\text{Na}_4[\text{Ru}(\text{TSPP})(\text{CO})(\text{DMF})] \cdot 2\text{DMF} \cdot 2\text{H}_2\text{O}$ (0.060 g, 5.22 mmol) was dissolved in DMSO (30 mL), by warming and sonicating the mixture. The solution was then syringed into a cooled photolysis cell and was photolyzed for 41-48 hours, under a stream of argon. The solution was concentrated under vacuum (2 mL), and the product was then precipitated from the ice-cooled solution by the addition of acetone (5 mL, dried over 4\AA sieves). The dark purple precipitate was collected on a frit and was then redissolved in a minimum amount of DMSO (2 mL). The solvent was then removed *in vacuo*. The dark purple product was shaken with hexanes and collected on a frit (the purple solid was extremely hygroscopic and was protected from atmospheric moisture). The dark purple crystalline product was then dried overnight at 100°C *in vacuo* (0.050 g, 74% yield). Isolated crystals were submitted for X-ray crystallographic analysis but were found to be twinned. Anal. Calcd for $\text{C}_{48}\text{H}_{66}\text{N}_4\text{Na}_4\text{O}_{29}\text{RuS}_6$ (i.e. $\text{Na}_4[\text{Ru}(\text{TSPP})(\text{DMSO})_2] \cdot 15\text{H}_2\text{O}$): C, 37.23; H, 4.30; N, 3.62. Found: C, 37.07; H, 4.35; N, 3.67. ^1H NMR (d_6 -DMSO, 300 MHz) δ 8.40 (s, 8H, pyrrole-H), 8.02 (d, 8H, $J_{\text{HH}'} = 7.5$ Hz, *m*- $\text{C}_6\text{H}_4\text{SO}_3^-$), 7.98 (d, 8H, $J_{\text{HH}'} = 7.5$ Hz, *o*- $\text{C}_6\text{H}_4\text{SO}_3^-$), 3.34 (br s, 30H, H_2O); ^1H NMR (D_2O , 500 MHz) δ 8.60 (s, 8H, pyrrole-H), 8.23 (d, 8H, $J_{\text{HH}'} = 7.5$ Hz, *m*- $\text{C}_6\text{H}_4\text{SO}_3^-$), 8.08 (d, 8H, $J_{\text{HH}'} = 7.5$ Hz, *o*- $\text{C}_6\text{H}_4\text{SO}_3^-$), -1.65 (s, 12H, bound-

[†] For convenience, the tetrasodium salt is sometimes written as $\text{Ru}(\text{TSPP})(\text{DMSO})_2^{4-}$.

OS(CH₃)₂) (see Section 3.6.1). IR (DMSO) ν_{SO} 1006 cm⁻¹. UV/visible data are given in Table 2.1.

(b) Thermolysis

Na₄[Ru(TSPP)(CO)(DMF)]·2DMF·2H₂O (0.005 g, 4.35×10^{-6} mol) in *d*₆-DMSO (0.6 mL) in an NMR tube was heated in an oil-bath to 120-130 °C for 50 hours. The ¹H NMR spectrum showed that the reaction had gone to completion (see Section 3.6.2); the bis-*d*₆-DMSO compound had most probably been formed because the *in situ* ¹H NMR spectrum was identical to that given above in (a).

Table 2.1: UV/visible data for the free-base porphyrins and the ruthenium(II) porphyrins

Compound	Soret [nm (log ϵ)]	Q Band(s) [nm (log ϵ)]
H ₂ (TSPP) ⁴⁻ a	414 (5.59)	516 (4.06), 552 (3.63), 580 (3.61), 634 (3.25)
H ₂ (TMPyP) ⁴⁺ b	419 (5.39)	515 (4.17), 553 (3.81), 586 (3.81)
H ₂ (TPyP) ^c	416	512, 544, 584, 644
H ₂ (TPP) ^d	417 (5.63)	514 (4.25), 549 (3.88), 591 (3.83), 650 (3.79)
Ru(TSPP)(CO)(DMF) ⁴⁻ e	412 (5.37)	530 (4.27)
Ru(TSPP)(CO)(DMF) ⁴⁻ e'	414	534
Ru(TSPP)(DMSO) ₂ ⁴⁻ f	412 (5.37)	516 (2.89)
"Ru(TMPyP)" g	420	534
"Ru(TPyP)" g	430	544, 588 sh
"Ru(TPP)" g	412	530, 564 sh

a. In H₂O; 1.30×10^{-5} mol L⁻¹; the data are in excellent agreement with those in the literature.^{4a,7}

b. In H₂O; 10^{-5} mol L⁻¹; the data are in excellent agreement with those in the literature.⁵

c. In DMF; the data are in excellent agreement with those in the literature^{4b} (the ϵ values are not given because the compound was impure).

d. In CHCl₃; 1×10^{-5} mol L⁻¹; the data are in excellent agreement with the literature.^{4b}

e. In H₂O; 10^{-6} - 10^{-5} mol L⁻¹; the data correspond to those of Ru(TSPP)(CO)(DMF)⁴⁻ prepared by method (a) and method (b) (see Section 2.5.1).

e'. *In situ* in DMF; the data correspond to those of Ru(TSPP)(CO)(DMF)⁴⁻ prepared by method (a) and method (b) (see Section 2.5.1).

f. In H₂O; 10^{-6} - 10^{-5} mol L⁻¹.

g. *In situ* (see Sections 2.5.2, 2.5.3 and 2.5.4); the nature of the species (including axial ligands) is unknown (see Section 3.5).

2.7 References

- (1) Pacheco-Olivella, A. A. M. Sc. Thesis, University of British Columbia, 1986.
- (2) Little, R. G.; Anton, J. A.; Loach, P. A.; Ibers, J. A. *J. Heterocyclic Chem.* **1975**, *12*, 343.
- (3) Pasternack, R. F.; Huber, P. R.; Boyd, P.; Engasser, G.; Francesconi, L.; Gibbs, E.; Fasella, P.; Venturo, G. deC.; Hinds, L. *J. Am. Chem. Soc.* **1972**, *94*, 4511.
- (4) (a) Meng, G. G.; James, B. R.; Skov, K. A.; Korbelik, M. *Can. J. Chem.* **1994**, *72*, 2447.
(b) Meng, G. G.; James, B. R.; Skov, K. A. *Can. J. Chem.* **1994**, *72*, 1894.
- (5) Ravensbergen, J. A. M. Sc. Thesis, University of British Columbia, 1993.
- (6) Srivastava, T. S.; Tsutsui, M. *J. Org. Chem.* **1973**, *38*, 2103.
- (7) Meng, G. Ph. D. Thesis, University of British Columbia, 1993.
- (8) Bruce, M. I. *J. Chem., Soc., Dalton Trans.* **1983**, 2365.
- (9) Evans, I. P.; Spencer, A.; Wilkinson, G. *J. Chem. Soc. Dalton Trans.* **1973**, 204.
- (10) Ludi, A. Personal communication to B. R. James.

Chapter 3: Results and Discussion

3.1 General Background

Porphyrins are aromatic macrocycles containing a conjugated system of 18π electrons. In their deprotonated form they belong to a much larger family of macrocyclic, quadridentate, anionic imine ligands that are very common in coordination chemistry; other examples include the phthalocyanine and bis-dimethylglyoxime ligands.¹ The carbon atoms in the porphyrin core are systematically numbered 1-20 (Fig. 3.1). The four carbon atoms between the pyrrole structures, are numbered 5, 10, 15 and 20 and are said to be in the *meso*-position.²

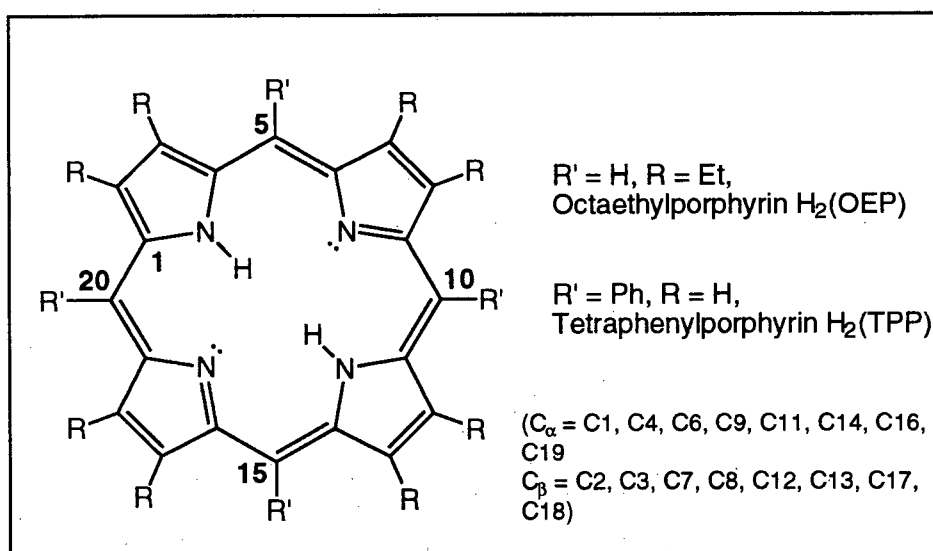


Figure 3.1: Generalized porphyrin structure.

A metalloporphyrin is formed when at least one of the central nitrogen atoms of the porphyrin core binds to a metal centre. Formally, metalloporphyrins may be considered as a metal complex of two amide, R_2N^- , and two imine ligands, giving a total electron count of eight electrons donated by the ligand.¹ Porphyrins have been found to bind to all common transition-metals of the periodic table. Methods of synthesis, however, have so far been rather haphazard. A directed, rational synthesis of early transition-metal porphyrins has

recently appeared in the literature which uses the alkali-metal porphyrins, $\text{Li}_2(\text{OEP})(\text{THF})_4$ and $\text{Na}_2(\text{OEP})(\text{THF})_4$ as metathesis reagents for ScCl_3 and ZrCl_4 .³⁻⁵

3.2 Ruthenium Metalloporphyrins

The first ruthenium metalloporphyrin was synthesized in 1969 and reported as $[\text{Ru}(\text{TPP})\text{Cl}(\text{CO})]$,⁶ although the correct oxidation state of the Ru and formulation of the complex as $\text{Ru}(\text{TPP})\text{CO}$ was not discovered until two years later.⁷ Currently, almost all synthetic methods for the insertion of Ru into porphyrins are based on modifications of the original procedures.⁶⁻⁸ These all produce stable Ru(II) carbonyl complexes, which are formed by the interaction of the free base porphyrin, $\text{H}_2(\text{porphyrin})$, with the ruthenium precursors $\text{Ru}_3(\text{CO})_{12}$, $\text{RuCl}_3 \cdot 3\text{H}_2\text{O}$ or $[\text{RuCl}_2(\text{CO})_3]_2$, either in the presence or the absence of a CO atmosphere. The thermolysis of $\text{Ru}_3(\text{CO})_{12}$ in the presence of a porphyrin is the most common method of synthesis. However the mechanism of the reaction which involves an oxidation of Ru(0) to Ru(II) is unclear.

The synthetic aim of this work was to metallate water-soluble porphyrins with ruthenium. A variety of porphyrins incorporating hydrophilic moieties may be routinely prepared: e.g. $\text{H}_2(\text{TSPP})^{4-}$ is prepared by electrophilic aromatic substitution of $\text{H}_2(\text{TPP})$. The water-soluble porphyrins used here are $\text{H}_2(\text{TSPP})^{4-}$ and $\text{H}_2(\text{TMPyP})^{4+}$ as shown in Figure 3.2, and are prepared as their sodium and tosylate salts, respectively. The free-base porphyrin, $\text{H}_2(\text{TSPP})^{4-}$, synthesized in this work, corresponded to the formula $\text{Na}_4[\text{H}_2(\text{TSPP})] \cdot 3\text{H}_2\text{O}$ which differed from a literature formulation of $\text{Na}_4[\text{H}_2(\text{TSPP})] \cdot 10\text{H}_2\text{O}$ for work from this group.⁹ Also the Soret and Q bands in the UV/visible spectrum for the trihydrate (Table 2.1) compared to those of the literature compound⁹ are each red-shifted by 3 nm. There is only one preparation known in the literature^{10a †} involving the formation of a

† Ru(II) porphyrins that are soluble in organic solvents have been made soluble in aqueous media by subsequent chemical reaction.^{10b}

water-soluble Ru porphyrin: the metallation of $\text{H}_2(\text{TSP})^{4-}$ with $\text{Ru}_3(\text{CO})_{12}$, which was repeated for comparison purposes.

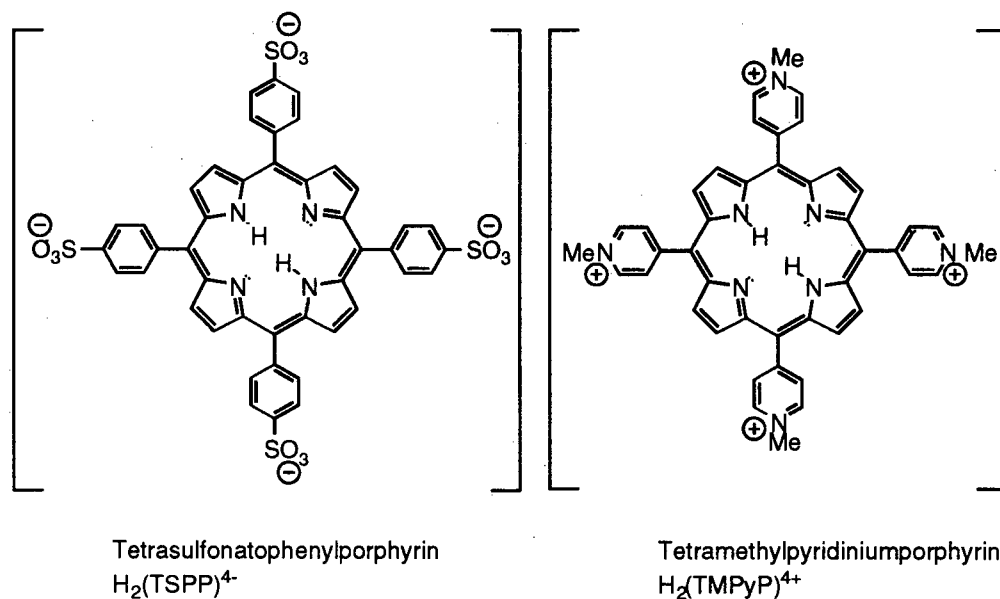


Figure 3.2: Water-soluble porphyrins.

3.3 Syntheses of Water-Soluble Ru Porphyrins

3.3.1 $\text{Ru}_3(\text{CO})_{12}$ precursor

The reported preparation¹⁰ involved the reaction of $\text{Ru}_3(\text{CO})_{12}$ with $\text{Na}_4[\text{H}_2(\text{TSP})] \cdot 12\text{H}_2\text{O}$ in a 3:1 ratio of Ru to porphyrin, in DMF at reflux for 1-3 weeks, under an atmosphere of argon or nitrogen. Upon metallation, the four Q bands observed by UV/visible spectroscopy are reduced to one (Table 2.1) and the inner pyrrole proton peak (-2.95 ppm) observed by ^1H NMR spectroscopy disappears. Both UV/visible and ^1H NMR spectroscopy are good diagnostic tools to judge the completion of the metallation reactions. The fact that the N-H peak appears so far upfield in the ^1H NMR spectrum is due to the shielding effects of the diamagnetic ring current induced in an aromatic ring in the presence of an applied magnetic field. As in the literature report, 1-3 weeks were needed to complete the metallation. However, all other findings were different. The method of purification had

to be modified because the compound could not be eluted down a column of either silica or alumina using $\text{CHCl}_3/\text{MeOH}$ as reported, but was purified instead by dialysis. The isolated, characterized, compound exhibited UV/visible absorptions in DMF, and an infrared spectrum that were different to those reported in the literature. Also, the compound was insoluble in CHCl_3 , so a UV/visible spectrum could not be taken in this solvent, whereas such a UV/visible spectrum was reported for the literature compound. By a painstaking process of dialysis and prolonged drying, pure material could be obtained corresponding to a formula of $\text{Na}_4[\text{Ru}(\text{TSPP})(\text{CO})(\text{DMF})]\cdot 6\text{H}_2\text{O}$ (see Section 2.5.1 method (a)). The literature formulation was given as $\text{Ca}_2[\text{Ru}(\text{TSPP})\text{CO}]\cdot 12\text{H}_2\text{O}$ (after the 4 Na^+ of an isolated, impure $\text{Na}_4[\text{Ru}(\text{TSPP})(\text{CO})]$ had been replaced with Ca^{2+} using CaCl_2), which was stated to be supported by “satisfactory elemental analysis”.

Under the same conditions, the metallations of $\text{H}_2(\text{TPyP})$ and $\text{H}_2(\text{TMPyP})^{4+}$ were attempted under N_2 or CO , but both the reactions were unsuccessful; also attempted was the metallation of $\text{H}_2(\text{TSPP})^{4-}$ with a 1:1 ratio of porphyrin to metal, but the reaction did not reach completion.

The procedure involving $\text{Ru}_3(\text{CO})_{12}$ was not a satisfactory method of metalloporphyrin synthesis for the following reasons: lengthy reaction times, the required preparation (usually with high CO pressure) of $\text{Ru}_3(\text{CO})_{12}$, and the metallation appeared limited to $\text{H}_2(\text{TSPP})^{4-}$. A different Ru precursor was sought that would alleviate one if not all of the problems associated with the $\text{Ru}_3(\text{CO})_{12}$ procedure.

3.3.2 *Cis*- $\text{RuCl}_2(\text{DMSO})_4$ and $[\text{Ru}(\text{DMF})_6](\text{OTf})_3^\dagger$ precursors

Water-soluble *cis*- $\text{RuCl}_2(\text{DMSO})_4$ was prepared¹¹ and failed to insert Ru into the water-soluble porphyrins under various conditions (e.g. $\text{H}_2(\text{TMPyP})^{4+}$ was heated at reflux in water with *cis*- $\text{RuCl}_2(\text{DMSO})_4$, in air for 24 hours). During the course of this thesis work the

[†] All the metallation reactions had to be carried out in the dark as the $\text{Ru}(\text{III})$ precursor is light-sensitive.

synthetic details for the Ru(III) compound $[\text{Ru}(\text{DMF})_6](\text{OTf})_3$ became available and it was made by the action of $\text{Pb}(\text{OTf})_2$ upon RuCl_3 in DMF.¹² The synthesis involved some modifications to the communicated procedure;¹² filtration to remove all the PbCl_2 salts was carried out through a layer of Celite and this was repeated until no more salts were collected, and also the mixture was cooled to 4 °C to precipitate out the crude product with 1,2- $\text{C}_2\text{H}_4\text{Cl}_2$. The yield of the reaction was less than half of that reported (48 %),¹² but the final product gave the simple formula of $[\text{Ru}(\text{DMF})_6](\text{OTf})_3$ (see Section 2.4.3) which was different to the reported, less attractive formulation of $[\text{Ru}(\text{DMF})_6](\text{OTf})_3 \cdot 0.25\text{CH}_2\text{Cl}_2 \cdot 0.1\text{C}_5\text{H}_{11}\text{OH}$.¹² The Ru(II) species, $[\text{Ru}(\text{DMF})_6](\text{OTf})_2$, can also be accessed by reducing the Ru(III) compound by dihydrogen in the presence of platinum black.¹² The Ru(II) species can also be obtained by reducing the Ru(III) compound in DMF in the presence of hydrogen alone. The colour change of the solution from pale yellow to pale red indicated that the reduction had occurred.¹² On exposure to air, the solution turned black (i.e. decomposition had occurred, as the Ru(II) species is air-sensitive). The relatively weakly coordinating dimethylformamide ligands offered the promise of easy displacement and various metallation reactions were attempted. With a 3:1 molar ratio of $[\text{Ru}(\text{DMF})_6](\text{OTf})_3$ and $\text{H}_2(\text{TSPP})^{4-}$ in DMF under 1 atm hydrogen, metallation fails to occur with or without heat. However, metallation does occur in the absence of hydrogen (under nitrogen) with a 3:1 ratio in DMF at reflux as before using $\text{Ru}_3(\text{CO})_{12}$. The reaction was complete in 3 hours and the spectroscopic data showed that the product (except for differences in solvation) was identical to that isolated previously (Sections 3.3.1 and 2.5.1 method (a)). Purification of the dark red product is simplified by dissolving the crude material in a minimum amount of DMF and then adding acetone and CH_2Cl_2 (see Section 2.5.1 (b)), which gives a pure, dark purple precipitate of $\text{Ru}(\text{TSPP})(\text{CO})(\text{DMF}) \cdot 2(\text{DMF}) \cdot 2\text{H}_2\text{O}$ (1) in 25% yield (see Section 3.4).

Under the same conditions, the reaction was performed with 2:1 and 1:1 ratios of Ru to $\text{H}_2(\text{TSPP})^{4-}$; however both of these reactions failed to reach completion. Metallation

reactions were also attempted with this Ru precursor and $\text{H}_2(\text{TSPP})^{4-}$, in water (at reflux under nitrogen or in air) and in DMSO (at reflux under nitrogen). In the former reaction, $\text{H}_2(\text{TSPP})^{4-}$ was protonated to give a species such as, $\text{H}_4(\text{TSPP})^{2-}$ (as judged by changes in the UV/visible spectra; the spectrum contained a Soret band at $\lambda_{\text{max}} = 434 \text{ nm}$ and a Q band at $\lambda_{\text{max}} = 646 \text{ nm}$, while this reverted to the original spectrum of $\text{H}_2(\text{TSPP})^{4-}$ upon the addition of triethylamine); in the latter no reaction occurred. The protonation of the porphyrin in water must result from increased acidity of the aqueous solution. This is perhaps produced when the Ru(III) precursor compound is firstly hydrated to form $\text{Ru}(\text{H}_2\text{O})_6^{3+}$, which would likely hydrolyse to generate $\text{Ru}(\text{H}_2\text{O})_{6-n}(\text{OH})_n^{(3-n)+}$ and H_3O^+ .

The successful metallation reaction involves a formal one-electron reduction from Ru(III) to Ru(II). The reductant is proposed to be CO,¹³ which derives from the decomposition of DMF, and which functions via the following half-equation with water that is present (eq 3.1):



Given the difficulty of metallating porphyrins with other Ru(II) precursors and the facility in metallating $\text{H}_2(\text{TSPP})^{4-}$ with $[\text{Ru}(\text{DMF})_6](\text{OTf})_3$ it is tentatively proposed that Ru^{3+} might first insert into the porphyrin cavity and then be reduced to Ru(II) by the above redox couple, perhaps mediated by a dimeric intermediate, bridged by a CO group. One observation that supports this hypothesis is the attempted metallation of $\text{H}_2(\text{TSPP})^{4-}$ by $[\text{Ru}(\text{DMF})_6](\text{OTf})_3$ in the presence of dihydrogen: the colour change from a dark purple solution to a dark brown solution suggested that the Ru(III) was reduced and decomposed before it complexed with the porphyrin. This result may also be rationalized on the basis of elementary coordination chemistry whereby the smaller, more electropositive Ru^{3+} ion would be more likely to insert into the restricted porphyrin cavity than Ru^{2+} . The reduction of Ru(III) to Ru(II) during the metallation was an unexpected bonus. With regard to the reduction, a dimeric intermediate must be predicated in order to satisfy the stoichiometry of the above half-equation (eq 3.1),

which gives a two-electron reduction that is not expected to proceed in two separate one-electron steps. Certainly Ru(III) porphyrin dimers are known (e.g. $[\text{Ru}_2(\text{OEP})_2]^{2+}$)¹⁴ but further evidence to support this mechanism is required.

3.4 Structure of $\text{Na}_4[\text{Ru}(\text{TSPP})(\text{CO})(\text{DMF})]$ (1)

The solution structure of $\text{Ru}(\text{TSPP})(\text{CO})(\text{DMF})^{4-}$ may be inferred from the variable temperature 500.13 MHz ^1H NMR spectrum of the complex (Fig. 3.3). Instead of an expected single sharp $[\text{AB}]_2$ resonance for the phenyl protons (e.g. if there is free rotation about the $\text{C}_{\text{meso}}\text{-C}_{\text{phenyl}}$ bond), broader peaks are observed: 2 doublets and an apparent triplet in a 1:1:2 ratio. This observation may be rationalized if it is assumed that the plane of the phenyl ring is canted to the plane of the porphyrin ring by some angle such that each *ortho* and *meta* proton resides in a different chemical environment as shown in Figure 3.4 (i.e. the upper and lower faces of the porphyrin are rendered inequivalent by the presence of two different axial substituents at the Ru). If values of $^4J_{\text{HH'}}$ are negligible then a doublet for each individual phenyl proton should be observed due to $^3J_{\text{HH'}}$ coupling between *ortho* and *meta* protons (i.e. an ABCD spin system). The observed triplet is thought to be due to an overlapping pair of doublets.

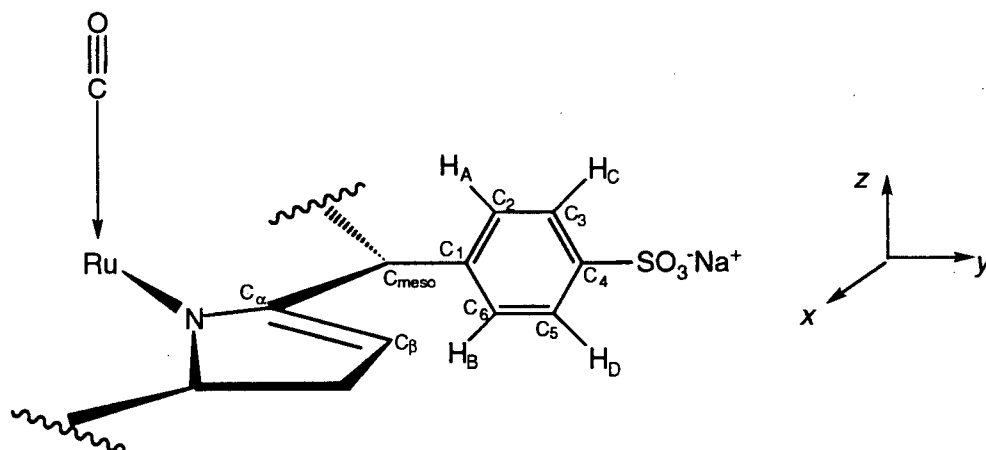


Figure 3.4: Different chemical environments for the phenyl protons in 1.

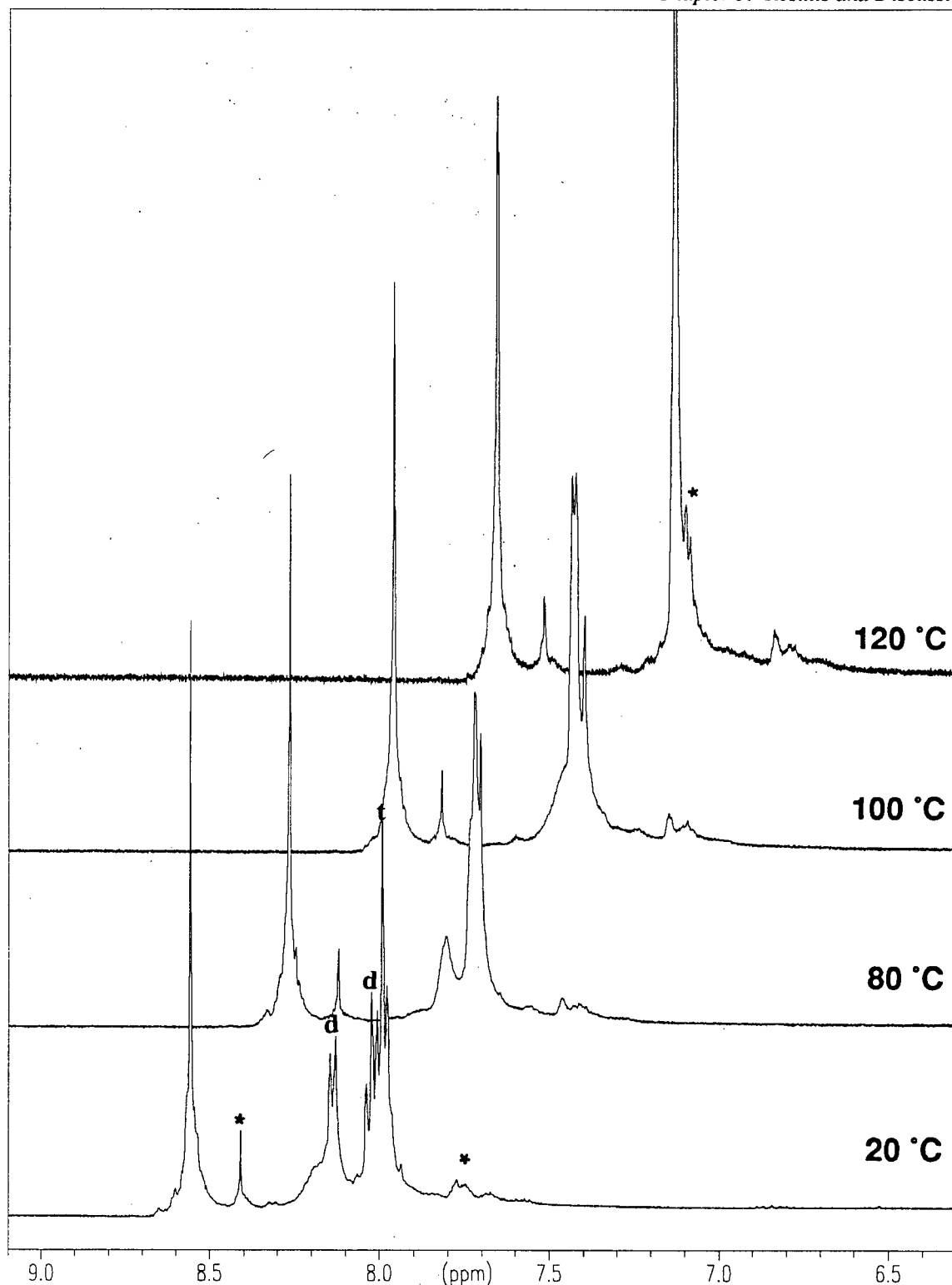


Figure 3.3: Variable temperature ^1H NMR of $\text{Na}_4[\text{Ru}(\text{TSPP})(\text{CO})(\text{DMF})]\cdot 2\text{DMF}\cdot 2\text{H}_2\text{O}$ (**1**) in d_6 -DMSO; the doublets (d) and triplet (t) assignments are described in the text. This is a stacked plot and does not represent a change in chemical shift with temperature. The signals marked with an asterisk correspond to small amounts of the thermolysis product $\text{Ru}(\text{TSPP})(\text{DMSO})_2^{4-}$ (see Sections 2.6 (b) and 3.6.2).

By analogy with data for $\text{H}_2(\text{TSPP})^{4-}$ and the sodium salt of benzene sulfonic acid^{9,15}, it is possible to assign the downfield peaks at 8.14 and 8.05 ppm to the *meta* protons H_C and H_D , and the upfield peaks at 7.99 ppm to the *ortho* protons H_A and H_B (the overlapping pair of doublets). The barrier to rotation may be overcome by heating the sample, and the inferred ABCD spectrum coalesces at 120 °C to a singlet resonance. At higher temperatures, rotation of the phenyl ring around the porphyrin becomes more facile so that each *ortho* and *meta* environment is interchanged rapidly. The chemical shift difference between the *ortho* and *meta* protons is too small to be resolved at 120 °C and a singlet results rather than an $[\text{AB}]_2$ resonance which is observed for similar systems at 99 °C (e.g. $\text{Ru}(4\text{-}i\text{PrTPP})\text{CO}$).¹⁶ This behaviour in solution is further evidence for a mono-CO Ru porphyrin versus a bis-CO system. A porphyrin with D_{4h} symmetry, such as provided by the structure of $\text{Ru}(\text{TPP})(\text{CO})_2$, would give a single symmetric $[\text{AB}]_2$ pattern in the ^1H NMR spectrum at all temperatures.

The $^{13}\text{C}\{^1\text{H}\}$ NMR spectroscopic data (see Section 2.5.1 method (b) and appendix II), are based on those assigned for $\text{Zn}(\text{TPP})$.¹⁷ The only significant difference between **1** and $\text{Zn}(\text{TPP})$ was found for C_α (which is clearly affected by the presence of the CO group) and the carbon directly attached to the sulfonate on the phenyl ring (C_4) (see Fig. 3.4). A singlet was observed for C_α at 147.4 ppm for **1** versus 151 ppm for $\text{Zn}(\text{II})\text{TPP}$, and for C_4 at 142 ppm for **1** versus 128 ppm for $\text{Zn}(\text{II})\text{TPP}$. An APT pulse sequence was performed which confirmed these assignments. The carbonyl resonance was difficult to detect in the $^{13}\text{C}\{^1\text{H}\}$ NMR spectrum, so an NMR sample was prepared under 2 atm of ^{13}CO which resulted in substantial signal enhancement. The CO resonance became the largest peak in the spectrum while the other carbon resonances in the spectrum remained unchanged. Separate signals were observed for the carbonyl species and for the uncoordinated ^{13}CO in d_6 -DMSO at 179 ppm and 184 ppm, respectively. The $^{13}\text{C}\{^1\text{H}\}$ NMR spectrum again indicates that there was only one type of CO complex present and as there were no changes

observed in the ^1H NMR spectrum, this would further support the evidence for the mono-CO complex. More forcing conditions were obtained by putting the sample of **1** under 20 atm of CO in d_6 -DMSO in a sapphire NMR tube. The resulting ^1H NMR spectrum was the same as for **1** under normal conditions.

These results indicate that the CO bound to Ru in **1** is labile to substitution by ligands of comparable donating ability (i.e. easy displacement of ^{12}CO by ^{13}CO), and that **1** will resist further substitution by CO to give a bis-CO complex. The electronic environment provided by the TSPP ligand to the Ru nucleus is therefore quite different to the environment provided by neutral porphyrins such as $\text{H}_2(\text{TPP})$ or $\text{H}_2(\text{OEP})$ systems. Ru bis-carbonyl species have been prepared with $\text{H}_2(\text{OEP})$ and $\text{H}_2(\text{TPP})$ ¹⁸ and the evidence seems to suggest that the more electron-rich the porphyrin the more stable the bis-CO porphyrin complex. On this basis, $\text{H}_2(\text{TSPP})^{4-}$ may be considered even more electron-poor than $\text{H}_2(p\text{-CF}_3\text{-TPP})$ for which a Ru bis-CO species has been inferred.^{18,19} The sulfonate groups on TSPP while each bearing a formal negative charge appear to withdraw electron density from the porphyrin ring.

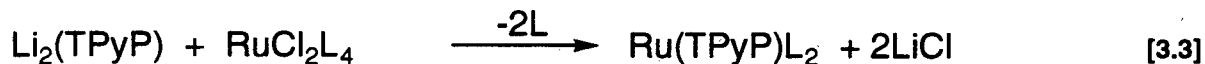
The elemental analyses of the product (**1**) correspond to the formula $\text{Na}_4[\text{Ru}(\text{TSPP})(\text{CO})(\text{DMF})]\cdot\text{solvate}$, where solvate = $2(\text{DMF})\cdot 2\text{H}_2\text{O}$ or $6\text{H}_2\text{O}$. The formulation of the mixed solvate species is supported by signals due to bound DMF, free DMF, and free H_2O , with the required integral ratio in the 300 MHz ^1H NMR spectrum (see for example, Section 2.5.1, method (b)) of samples prepared under nitrogen in anhydrous d_6 -DMSO. The NMR data also show that the axial DMF ligand is retained in this medium. The solid state IR spectrum of **1** shows three ν_{CO} stretches (see Section 2.5.1, the IR spectrum (method b) is given in Appendix I), which could indicate either the presence of more than one mono-CO complex (e.g. with H_2O as the axial ligand), a trace of some Ru-CO impurity or solid state effects. Solution IR measurements in DMSO gave a value of 1913 cm^{-1} for the carbonyl stretching frequency, a value consistent with a mono-CO species.¹⁸ Bis-CO species

typically have carbonyl stretching frequencies of 1990-2050 cm^{-1} , which reflects the smaller degree of back donation into the two competing *trans* carbonyl ligands.¹⁸

3.5 Other Ruthenium Porphyrins

$[\text{Ru}(\text{DMF})_6](\text{OTf})_3$ may also be used to metallate $\text{H}_2(\text{TPyP})$, $\text{H}_2(\text{TPP})$ and $\text{H}_2(\text{TMPyP})^{4+}$ by a method equivalent to that used for **1**, which establishes the versatility of $[\text{Ru}(\text{DMF})_6](\text{OTf})_3$ in metallating anionic, cationic, and neutral porphyrins. “Ru(TPyP)” is likely a polymeric material as the red product obtained from the reaction was insoluble in every solvent tested. The formation of a polymer containing bridging Ru centres, linked to $\text{H}_2(\text{TPyP})$ via the nitrogen of the pyridyl group is conceivable.²⁰ “Ru(TPP)” and “Ru(TMPyP)” were synthesized on an NMR sample scale, successful metallations being indicated by the reduction of the Q bands (four and three respectively) observed by UV/visible spectroscopy to one (Table 2.1), and the disappearance of the inner pyrrole proton peak of $\text{H}_2(\text{TMPyP})^{4+}$ (-3.10 ppm) observed by ^1H NMR spectroscopy.

More ambitiously, the preparation of a $\text{Li}_2(\text{TPyP})$ species was attempted by an acid-base reaction between $\text{H}_2(\text{TPyP})$ and $\text{LiN}(\text{SiMe}_3)_2$ in THF as shown in eq 3.2, and as demonstrated for OEP systems by Arnold’s group.³ Given the success of this approach in early transition-metal porphyrin chemistry (cf. eq 3.3), a similar protocol was attempted for the synthesis of alkali metal porphyrins of $\text{H}_2(\text{TPyP})$ and of similarly substituted porphyrins. A suitable Ru(II) or Ru(III) halide precursor might then be used to metallate the Li or Na salt of $\text{H}_2(\text{TPyP})$ (eq 3.3). A neutral porphyrin such as $\text{H}_2(\text{TPyP})$ was used rather than a cationic or anionic porphyrin because of the capacity of these charged species to bind water molecules which would react firstly with $\text{LiN}(\text{SiMe}_3)_2$. Unfortunately, the $\text{Li}_2(\text{TPyP})$ species could not be accessed by these means and time constraints did not allow further evaluation of this metathesis reaction towards ruthenium.



3.6 Removal of the Axial CO Group from Ru(TSPP)(CO)(DMF) (1)

Several procedures established the efficient removal of the CO ligand from Ru(II) mono-carbonyl porphyrin complexes. These include: direct substitution of the CO group with a strongly coordinating ligand,^{7,21} photolysis in a suitably coordinating solvent,^{22,23} and oxidation to form *trans*-dioxo species or Ru(IV) μ -oxo binuclear species.^{24,25} In this work, photolysis was used as the method of choice.

3.6.1 Photolysis of 1

In DMSO solvent, photolysis removes the CO ligand from Ru(TSPP)(CO)(DMF)⁴⁻ (1) to give a new species **2** formulated as Ru(TSPP)(DMSO)₂⁴⁻. Completion of the photolysis reaction was strongly dependent on the concentration of **1**, and also on the intensity of the mercury vapour lamp. Upon removal of the DMSO, **2** was isolated as a dark purple crystalline material. Purification with acetone and removal of excess DMSO with hexanes gave material that analyzed as Na₄[Ru(TSPP)(DMSO)₂]·15H₂O. The formulation is supported by ¹H NMR signals due to bound DMSO (in a sample prepared in air in D₂O) and free H₂O with the required integral ratio (for a sample prepared under nitrogen in anhydrous *d*₆-DMSO). Normally, the ¹H NMR chemical shift can be used as a criterion to distinguish between O-bonded and S-bonded DMSO ligands, which results in a downfield shift from free DMSO of about 0.2 and 0.7 ppm, respectively.¹¹ In this complex, as the DMSO is axially bound, the ring current effect of the porphyrin shifts the methyl peak too far upfield (to -1.65 ppm) for this criterion to be applied. As expected for a symmetric metalloporphyrin structure with *D*_{4h} symmetry, the ¹H NMR spectrum of **2** features a sharp [AB]₂ resonance in the phenyl region (see Section 2.6 (a)).

The ν_{SO} of **2** was identified at 1006 cm^{-1} , which represents a bathochromic shift with respect to the ν_{SO} observed for free DMSO at 1055 cm^{-1} .^{26,27} Numerous studies have stated that a bathochromic shift indicates coordination through the oxygen atom to the metal centre whereas a hypsochromic shift (i.e. $\nu_{\text{SO}} > 1055\text{ cm}^{-1}$) indicates coordination through the sulfur atom.^{26,27} A simple rationalization may be drawn from the valence bond representation of bonding in free DMSO as shown in Figure 3.5. Canonical form **III** would be expected to predominate in the case of sulfur coordination thereby increasing the S-O bond order and resulting in a hypsochromic shift; canonical form **I** would be expected to predominate in the case of oxygen coordination, decreasing the S-O bond order likewise resulting in a bathochromic shift. On this basis, **2** contains oxygen-bonded DMSO ligands. Normally ligation through the sulfur atom might be expected for Ru(II), a second-row metal which occurs fairly late in the transition series. This expectation is in accord with the HSAB principle which holds that a softer base (the sulfur donor) would be more likely to coordinate to the soft acid Ru^{2+} than the harder oxygen donor.²⁷⁻²⁹ Such sulfur coordination is indeed observed in $\text{Ru}(\text{OEP})(\text{DMSO})_2$ ($\nu_{\text{SO}} = 1105\text{ cm}^{-1}$).³⁰ However oxygen coordination has been shown to occur in instances where a softer metal ion is bound to an electron-withdrawing ligand, thereby increasing the acidity of the metal and promoting oxygen donation (e.g. as in $[\text{Rh}(\text{DMSO})]_2(\mu\text{-O}_2\text{CCF}_3)_4$).³¹ Oxygen coordination can also occur if the DMSO ligand is sterically hindered: cf. *trans*- $\text{RuCl}_2(\text{DMSO})_4$ versus *cis*- $\text{RuCl}_2(\text{DMSO})_3(\text{DMSO})$.^{11,32,33} In **2**, if the TSPP ligand is considered to be relatively electron-withdrawing (e.g. vs. OEP), then the preference for oxygen coordination may be rationalized.

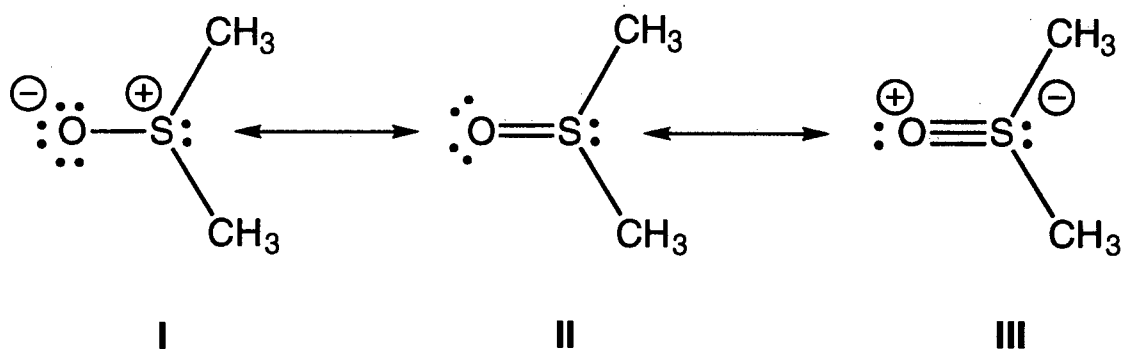


Figure 3.5: Canonical forms of DMSO.

3.6.2 Thermolysis of 1

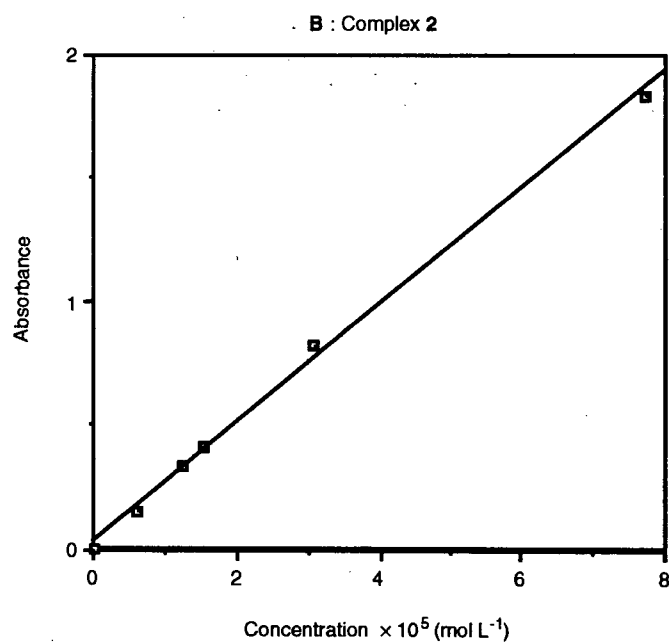
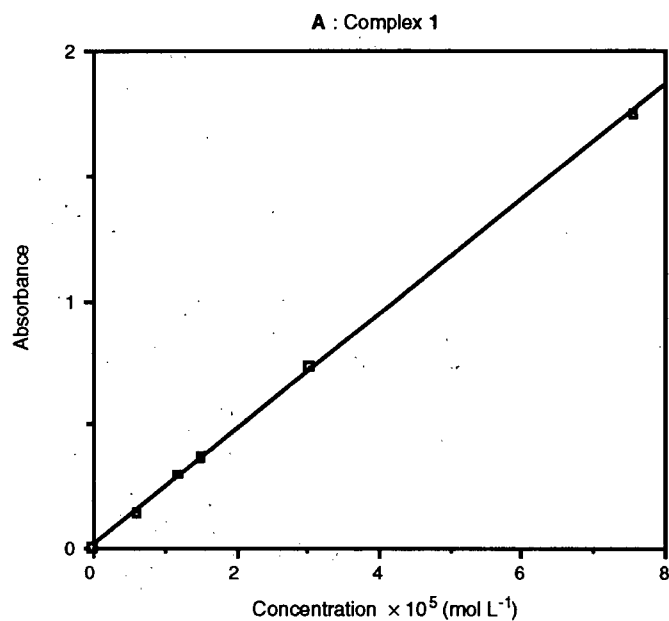
Complex **2** was also accessible by thermolysis of **1** in d_6 -DMSO at 120 °C after 50 hours. Thermolysis therefore offers an alternative route for CO removal in the presence of the relatively strong donor DMSO ligand.

3.7 Aggregation Studies

The aggregation of porphyrins was first observed as early as the 1930s,³⁴ and is often encountered in the studies of porphyrins in aqueous solution.³⁵ It occurs with the free-base porphyrin in solution as a result of the hydrophobic properties of the porphyrin ring. In aqueous solution, π - π interactions need only be considered.³⁶ There are many methods employed in the study of aggregation and these include: UV/visible and fluorescence spectroscopy,³⁷ temperature jump kinetic studies,³⁸ and NMR spectroscopy.³⁹ Aggregation has been consistently related to the deviation from the familiar Beer-Lambert law, and hence UV/visible spectroscopy is an excellent method for its detection.^{40,41} Also observable by this form of spectroscopy is the dispersion of aggregates in aqueous solution into their monomeric forms, this being promoted by the addition of an organic solvent, commonly methanol or ethanol.⁴²

Previous work^{39,43} has shown that $\text{H}_2(\text{TSPP})^{4-}$ aggregates in aqueous solutions over a concentration range of 10^{-6} to 10^{-4} mol L⁻¹. This has been shown by the fact that the measured molar absorptivity (ϵ) is not constant over a range of concentrations, and absorbance deviates significantly from Beer's law. It has also been shown that disaggregation is induced by the addition of methanol.⁴³ The work of Fleischer et al.⁴⁴ concludes that $\text{H}_2(\text{TSPP})^{4-}$ does not aggregate in aqueous solution (10^{-9} to 10^{-4} mol L⁻¹); however, past and present work in this laboratory⁴³ have consistently indicated the occurrence of aggregation for $\text{H}_2(\text{TSPP})^{4-}$. Studies have indicated that the aggregation of $\text{H}_2(\text{TSPP})^{4-}$ may occur via a monomer-dimer model, in which the dimeric structure is proposed to be in a "face to face" type arrangement.³⁷

The two ruthenium (II) porphyrins synthesized in this work and $\text{H}_2(\text{TSPP})^{4-}$ were examined for Beer's Law deviation by varying both the concentration and the percentage alcohol in the solvent. The Beer's law plots at the Soret maximum (412 nm) for the water-soluble Ru(II) porphyrins and the free-base porphyrin are shown in Figures 3.6, A, B, and C.



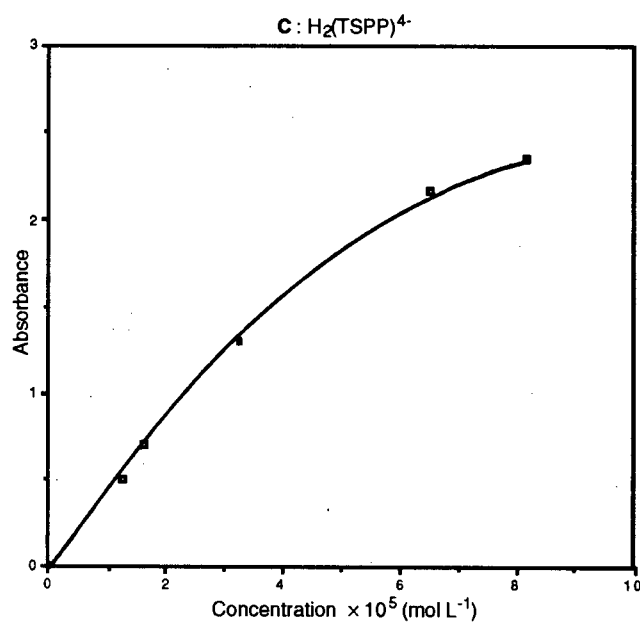


Figure 3.6: Beer's Law study of **A**: complex 1, **B**: complex 2, and **C**: $\text{H}_2(\text{TSPP})^{4-}$, in aqueous solution over a concentration range of 10^{-6} - 10^{-4} mol L⁻¹ in 0.1 cm and 1 cm cells.

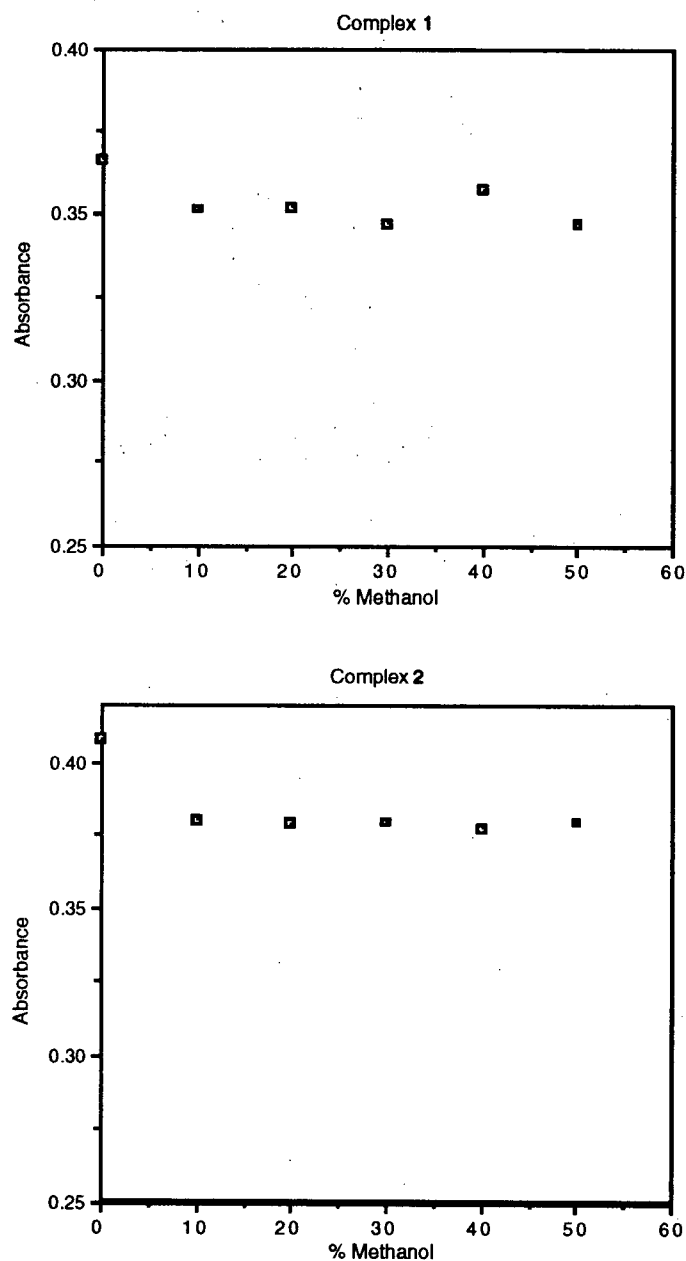


Figure 3.7: Aggregation study of 1 and 2 (concentration = 2.0×10^{-5} mol L⁻¹).

If aggregation occurs, significant deviation from linearity is expected. However, over the concentration range tested, for both Ru(II) porphyrin complexes(Figs 3.6, A, and B), no significant aggregation was observed. The extinction coefficient of 1 and 2 in water were

found to be 2.32×10^5 ($\log \epsilon = 5.37$) and $2.37 \times 10^5 \text{ L mol}^{-1} \text{ cm}^{-1}$ ($\log \epsilon = 5.37$) respectively, which are typical values for Soret bands of Ru(II) porphyrin complexes.¹⁶ Conversely, aggregation is clearly observed for $\text{H}_2(\text{TSPP})^{4-}$ over the concentration range 10^{-6} to $10^{-4} \text{ mol L}^{-1}$ (Fig. 3.6, C). Also, there was no change in absorbance at the Soret maxima for **1** and **2** at a concentration of $2.0 \times 10^{-5} \text{ mol L}^{-1}$ when the percentage methanol was varied (0-50 %), as shown in Figure 3.7. The aggregation study of **1** and **2** using methanol addition was also repeated at a lower concentration ($6 \times 10^{-7} \text{ mol L}^{-1}$), and again as expected aggregation was not apparent. These results may be compared with the literature findings that the free base porphyrin, $\text{H}_2(\text{TSPP})^{4-}$, aggregates over a comparable concentration range (10^{-6} to $10^{-4} \text{ mol L}^{-1}$) in aqueous solution.^{39,43} This difference in solution behaviour is undoubtedly due to the presence of axial ligands that are reasonably strongly bound to the metal centre. Ruthenium(II), when inserted into a porphyrin, adopts an octahedral geometry, and the presence of the axial ligands in **1** or **2** (DMF, H_2O , or DMSO) presumably prevents the close approach of the hydrophobic porphyrin planes and aggregation is therefore not observed.

3.7.1 Axial ligand substitution promoting aggregation/disaggregation

A UV/visible spectrum of **2**, in distilled water ($[\text{2}] = 1.24 \times 10^{-6} \text{ mol L}^{-1}$), gave a Soret band at 412 nm (with perhaps a slight shoulder at 394 nm). After the solution was heated to 74°C for 3.5 hours (the solution in the UV/visible cell was sealed in air), the resulting spectrum contained a Soret band at 410 nm that was broader and reduced in intensity (Fig. 3.8).

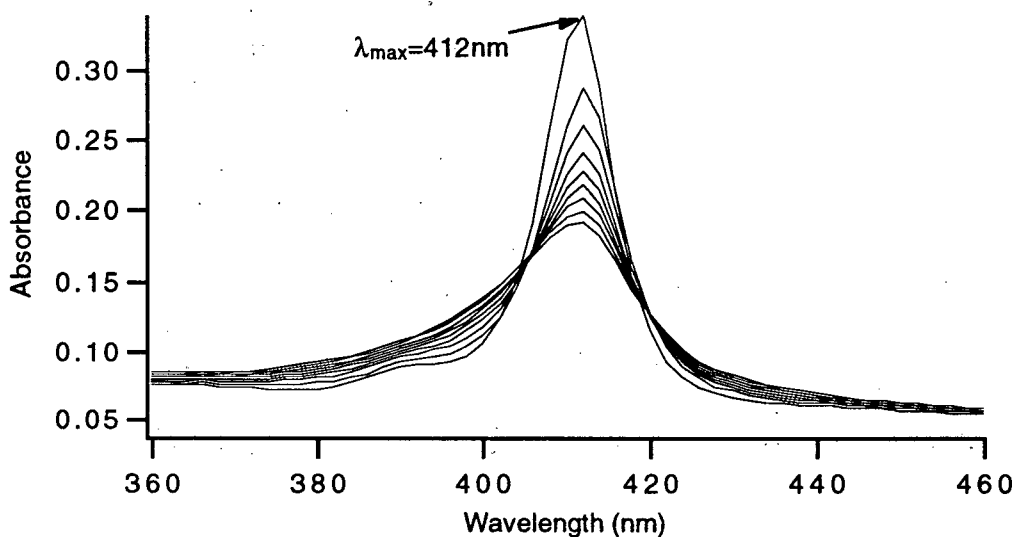


Figure 3.8: Soret band absorption change when **2** is heated in aqueous solution.

The presence of isosbestic points[†] at 406 nm and 420 nm indicated that a simple conversion reaction was occurring, most probably between two species. This may be axial ligand substitution to produce a mono- or possibly a bis-aqua species. Of note, on addition of DMSO (0.3 mL) to the solution (2.45 mL) at room temperature, the absorbance reverted slowly to the original spectrum of **2**, over a period of 2.5 hours (Fig. 3.9). The data are consistent with reversible formation, for example, of a mono-aqua species from **2** (eq 3.4).



[†] The “deviation” of the initial spectrum is because the solution had not yet reached the required temperature.

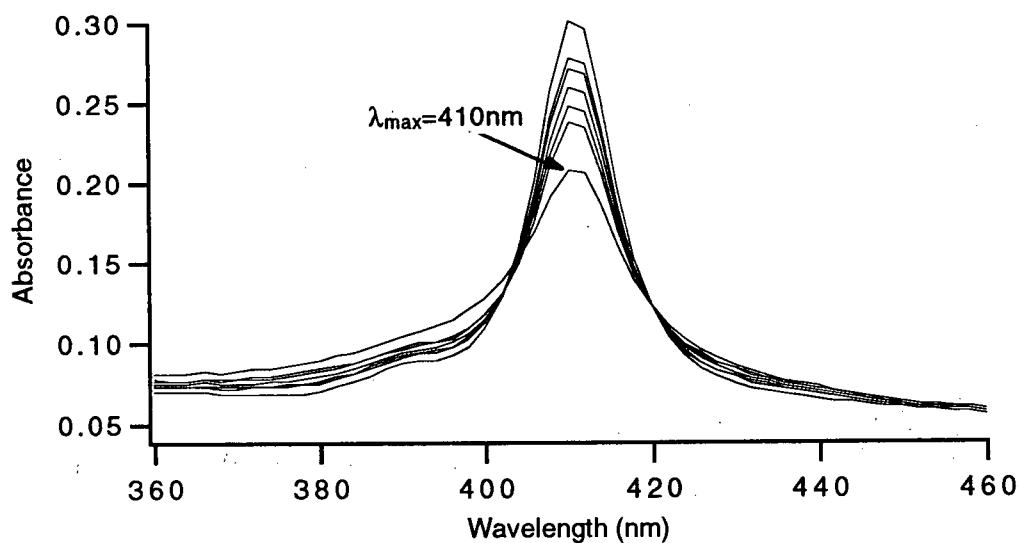


Figure 3.9: Soret band absorption change upon the addition of DMSO.

The same procedure was carried out at a higher concentration of **2** ($[2] = 9.11 \times 10^{-6} \text{ mol L}^{-1}$) which permitted the observation of the less intense Q band (Fig. 3.10). The Soret band again decreased in intensity to give a broad band at 410 nm, while the Q band shifted reversibly from 516 to 526 nm. This shift in the Q band also indicated that another species had been formed as this band is affected by the identity of the axial ligand (cf. $\text{Ru}(\text{TSPP})(\text{CO})(\text{DMF})_4^{4-}$ versus $\text{Ru}(\text{TSPP})(\text{DMSO})_2^{4-}$ (Table 2.1)).

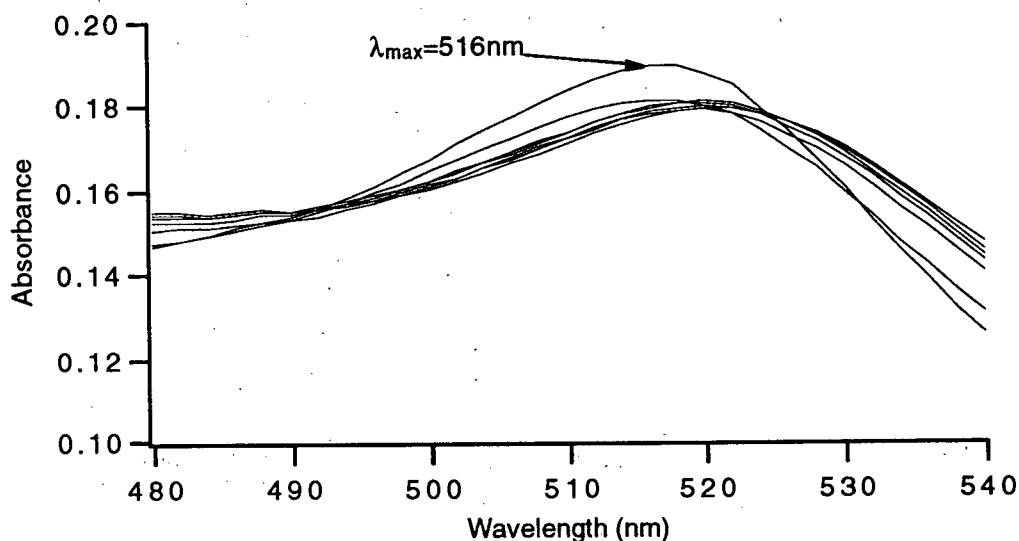


Figure 3.10: Q band absorption change when **2** is heated in aqueous solution (due to technical difficulties the final spectrum at $\lambda_{\text{max}} = 526 \text{ nm}$ could not be overlayed onto the graph).

Without further experimental evidence it is not possible to state whether the end-point of the substitution reactions results in the formation of the mono- or bis-aqua species although the former is considered more probable, because the existence of a second substitution process is less likely to result in an isosbestic system. If the bis-aqua species was formed, it could have the potential to aggregate via a H-bonding network. This could be reflected by the broadness of the resultant Soret band.⁴⁵ Therefore axial ligand substitution processes could promote aggregation and disaggregation.

3.8 References

- (1) Collman, J. P.; Hegedus, L. S.; Norton, J. R.; Finke, R. G. *Principles and Applications of Organotransition Metal Chemistry*; University Science Books: Mill Valley, California, 1987, p 182-183.
- (2) Bonnet, R. In *The Porphyrins*; D. Dolphin, Ed.; Academic Press: New York, 1978; Vol. I; p 2.
- (3) Brand, H.; Arnold, J. *J. Am. Chem. Soc.* **1992**, *114*, 2266.
- (4) Arnold, J.; Dawson, D. Y.; Hoffman, C. G. *J. Am. Chem. Soc.* **1993**, *115*, 2707.
- (5) Arnold, J.; Hoffman, C. G. *J. Am. Chem. Soc.* **1990**, *112*, 8620.
- (6) Fleischer, E. B.; Thorp, R.; Venerable, D. *J. Chem. Soc., Chem. Commun.* **1969**, 475.
- (7) Chow, B.; Cohen, I. *Bioinorg. Chem.* **1971**, *1*, 57.
- (8) Tsutsui, M.; Ostfield, D.; Hoffman, L. M. *J. Am. Chem. Soc.* **1971**, *93*, 1820.
- (9) Meng, G. G.; James, B. R.; Skov, K. A.; Korbelik, M. *Can. J. Chem.* **1994**, *72*, 2447.
- (10) (a) Pawlik, M.; Hoq, M. F.; Shepherd, R. E. *J. Chem. Soc., Chem. Commun.* **1983**, 1467.
(b) Hambright P., *Inorg. Chim. Acta* **1989**, *157*, 95.
- (11) Evans, I. P.; Spencer, A.; Wilkinson, G. *J. Chem. Soc. Dalton Trans.* **1973**, 204.
- (12) Ludi, A., Personal communication to B. R. James.
- (13) Sheldon R. *Chemicals from Synthesis Gas*; Reidel Publishing Co., Dordrecht, 1983; Chapter 2.
- (14) Collman, J. P.; Prodoliet, J. W.; Leidner, C. R. *J. Am. Chem. Soc.* **1986**, *108*, 2916.
- (15) *The Sadtler Handbook of Proton NMR Spectra*; Sadtler: Philadelphia, 1978, p 569.
- (16) Bonnet, J. J.; Eaton, S. S.; Eaton, G. R.; Holm, R. H.; Ibers, J. A. *J. Am. Chem. Soc.* **1973**, *95*, 2141.
- (17) Janson, T. R.; Katz, J. J. In *The Porphyrins*; D. Dolphin, Ed.; Academic Press: New York, 1978; Vol. IVb; p 46.
- (18) Eaton, G. R.; Eaton, S. S. *J. Am. Chem. Soc.* **1975**, *97*, 235.

- (19) Eaton, G. R.; Eaton, S. S. *Inorg. Chem.* **1976**, *15*, 134.
- (20) Shi, C.; Anson, F. C. *Inorg. Chim. Acta* **1994**, *225*, 215.
- (21) Sishta, C.; Camenzind, M. J.; James, B. R.; Dolphin, D. *Inorg. Chem.* **1987**, *26*, 1181, and references therein.
- (22) Hopf, F. R.; O'Brien, T. P.; Scheidt, W. R.; Whitten, D. G. *J. Am. Chem. Soc.* **1975**, *97*, 277.
- (23) Rajapakse, N.; James, B. R.; Dolphin, D. *Catalysis Letts.* **1990**, *55*, 109, and references therein.
- (24) Collman J. P.; Barnes C. E.; Brothers, P. J.; Collins, T. J.; Ozawa, T.; Gallucci, J. C.; Ibers, J. A. *J. Am. Chem. Soc.* **1984**, *106*, 5151.
- (25) Mlodnicka, T.; James, B. R. In *Metalloporphyrin Catalyzed Oxidations*; F. Montanari and L. Casella, Eds.; Kluwer Academic: Dordrecht, 1994; p 121.
- (26) James, B. R.; Morris, R. H.; Reimer, K. J. *Can. J. Chem.* **1977**, *55*, 2353.
- (27) Davies, J. A. *Adv. Inorg. Chem. Radiochem.* **1981**, *24*, 115.
- (28) Reynolds, W. L. *Prog. Inorg. Chem.* **1970**, *12*, 1.
- (29) *Hard and Soft Acids and Bases*; Dowden, Hutchinson & Ross Inc.: Stroudsburg, 1973.
- (30) Pacheco, A. Ph. D. Thesis, University of British Columbia, 1992; Pacheco A.; James B. R.; Rettig S. J. *Inorg. Chem.*, Submitted.
- (31) Cotton, F. A.; Felthouse, T. R. *Inorg. Chem.* **1980**, *19*, 2347.
- (32) Jaswal, J. S.; Rettig, S. J.; James, B. R. *Can. J. Chem.* **1990**, *68*, 1808.
- (33) Mercer, A.; Trotter, J. *J. Chem. Soc., Dalton Trans.* **1975**, 2480.
- (34) White, W. J. In *The Porphyrins*; D. Dolphin, Ed.; Academic Press: New York, 1978; Vol. V; p 304.
- (35) See reference 35; p 303.
- (36) Hunter, C. A.; Sanders, J. K. M. *J. Am. Chem. Soc.* **1990**, *112*, 5525.

- (37) Kano, K.; Miyake, T.; Uomoto, K.; Sato, T.; Ogawa, T.; Hashimoto, S. *Chem. Lett.* **1983**, 1867.
- (38) Pasternack, R. F.; Huber, P. R.; Boyd, P.; Engasser, G.; Francesconi, L.; Gibbs, E.; Fasella, P.; Venturo, G. C.; Hinds, L. deC. *J. Am. Chem. Soc.* **1972**, *94*, 4511.
- (39) Corsini, A.; Herrmann, O. *Talanta* **1986**, *33*, 335.
- (40) See reference 35; p 305.
- (41) See reference 35; p 332-333.
- (42) Gallagher, W. M.; Elliott, W. B. *Ann. N. Y. Acad. Sci.* **1973**, *206*, 463.
- (43) Meng, G. G. Ph. D. Thesis, University of British Columbia, 1993.
- (44) Fleischer, E. B.; Palmer, J. M.; Srivastava, T. S.; Chatterjee, A. *J. Am. Chem. Soc.* **1971**, *93*, 3162.
- (45) Paine J. B.; Dolphin, D.; Gouterman, M. *Can. J. Chem.* **1978**, *56*, 1713.

Chapter 4: Biological Tests

4.1 Introduction

One of the initial aims of this thesis work was to synthesize water-soluble ruthenium porphyrin compounds as potential radiosensitizers. To establish the *in vivo* potential of a drug, a variety of *in vitro* tests should initially be performed. In order for it to be effective, a radiosensitizing drug should be able to cross a cellular membrane, and, also, it should have the capacity to interact with DNA: the main target of cell kill in radiotherapy. Therefore any radiotherapy drug should have the ability to recognise and affect DNA in some way. The complex $\text{Ru}(\text{TSPP})(\text{CO})(\text{DMF})_4^+$ (1) was tested to see whether it would accumulate in, and be toxic to, CHO (Chinese Hamster Ovary) cells. It was also tested to see whether it would bind to DNA, by means of a plasmid binding assay, and whether the damaged DNA (1 bound to DNA) would be recognized by the so-called High Mobility Group protein (HMG), which has been shown to occur in the case of *Cis*-platin (see Section 4.4.2). This was tested for by the Damaged DNA Affinity Precipitation Assay (DDAP). The complex $\text{Ru}(\text{TSPP})(\text{DMSO})_2^+$ (2) was also tested in the plasmid binding study and for its radiosensitizing potential.

4.2 Cell Preparation

The cells used in the *in vitro* tests (Sections 4.3, 4.4, 4.5) were a CHO cell line. The cells were routinely grown in a spinner culture flask in α (+/+) medium, and the cell solutions were maintained at 37 °C in an "Incu-cover" incubator (Associated Biomedic Systems). The cell cultures were diluted daily to a cell concentration of about 1×10^5 cells mL^{-1} to maintain an exponential growth (doubling time was approximately 13 hours).

4.3 Cell Accumulation

The accumulation profile of **1** was determined in air by incubating CHO cells in 50-200 $\mu\text{mol L}^{-1}$ solutions of this compound, following a literature procedure.¹ A 500 $\mu\text{mol L}^{-1}$ solution of **1** was prepared in $\alpha(+/-)$ medium and was sterilized by filtration through a 0.22 micromillipore Nalgene filter. Three solutions (50, 100, 200 $\mu\text{mol L}^{-1}$) were then prepared from this stock solution by diluting each in various volumes of the $\alpha(+/-)$ medium, and a blank solution (0 $\mu\text{mol L}^{-1}$) was also tested. To each solution was then added 1 mL of CHO cells at 5×10^6 cells mL^{-1} to make four 20 mL solutions which were then incubated in air for 1 hour at 37 °C. Each solution (19 mL, the other 1 mL was used in the toxicity study) was then centrifuged with cooling (4 °C) at 600 rpm for 8 min and the supernatant containing excess extra-cellular ruthenium porphyrin was decanted. The cell pellet was resuspended in phosphate buffer saline solution (PBS) (10 mL) at 0 °C and was then vortexed to resuspend the cells. The washing procedure was then repeated to ensure the complete removal of any extra-cellular Ru complex. The cells were pelleted once again, the supernatant was decanted, and the cells were then resuspended in PBS (5 mL). A cell count was then taken (following dilution of 0.2 mL into 19.8 mL PBS) using a Coulter counter (Coulter Electronics). The cells were pelleted a final time and, once the supernatant was decanted, they were dried for 30 minutes and were then digested by occasional vortexing in 50 μL concentrated nitric acid at 37 °C for 2 hours. Once completely digested, the solutions were diluted by adding 250 μL water and were assessed for ruthenium content by the use of a Varian SpectrAA 300 spectrometer with a graphite tube atomizer (calibrated with the ruthenium standards (960 $\mu\text{g/mL}$) provided by Sigma).

4.3.1 Accumulation study of **1**

A graph of Ru accumulation in the CHO cells versus incubation concentration of **1** is shown in Figure 4.1. The accumulation profile (Fig. 4.1) clearly shows that complex **1** was entering the cell, though the actual amount of Ru, $(5.30 - 8.81) \times 10^{-6}$ ng Ru/cell is far less

than that found, for example, for *trans*-RuCl₂(*i*PrS(O)(CH₂)₂S(O)*i*Pr)₂, 175×10^{-6} ng Ru /cell over 4 hours.² It is, however, comparable to that found for *Cis*-platin ($10 \mu\text{mol L}^{-1}$), 2.43×10^{-6} ng Pt /cell for a 1 hour accumulation study.¹

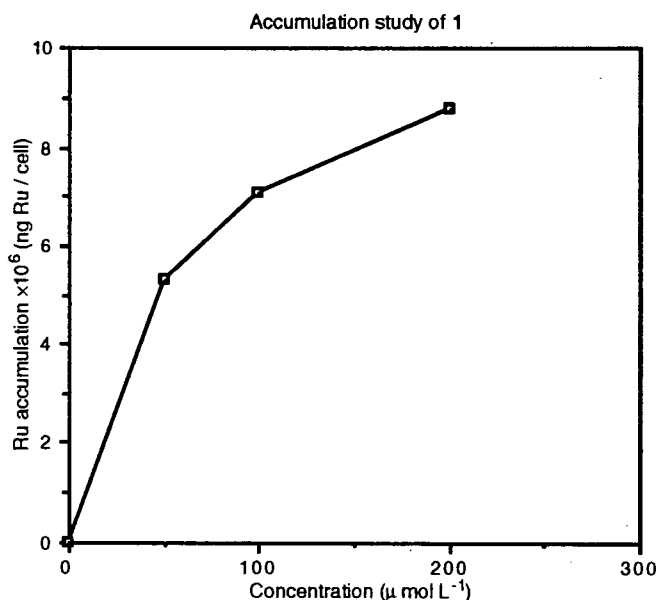


Figure 4.1: Accumulation of Ru from incubation of CHO cells with **1** ($50\text{-}200 \mu\text{mol L}^{-1}$) for 1 hour.

4.4 Toxicity

The toxicity of **1** was examined in air by comparing the plating efficiency (defined in eq 4.1) of cells incubated in the porphyrin solution compared to cells incubated in control solutions, following the literature procedure used for nitroimidazoles.³ A 1 mL sample of each solution incubated for the accumulation study (Section 4.3, $0\text{-}200 \mu\text{mol L}^{-1}$) was used in this study. Each sample was put into 9 mL of medium α (-/-) at 0°C and was placed in the centrifuge (600 rpm, 8 min). The supernatant was then decanted and the cells resuspended in

10 mL of fresh media $\alpha(-/-)$. The cells were counted (after dilution of 2 mL cell solution into 10 mL PBS) and were plated into Petri dishes with nutrient medium (5 mL, $\alpha(+/+)$) which had been equilibrated (solutions maintained 24 hours at 37 °C with a 95% air/ 5% CO₂ gas flow) in a tray incubator (National Inc.). The cells were grown for one week, at which time the colonies were stained with methylene blue (6 min), counted and compared to the original number of cells that were initially plated, and the plating efficiency (P.E.) was determined. The P.E. is simply the ratio of the number of colonies (defined as >50 cells) found after one week to the number of cells plated (eq 4.1):

$$\text{P. E.} = \frac{\text{Colonies Counted}}{\text{Cells Plated}} \quad [4.1]$$

4.2.1 Toxicity of **1** toward CHO cells

A toxicity study was carried out for **1** over a concentration range 50 - 200 $\mu\text{mol L}^{-1}$, and plating efficiencies were calculated and graphically arranged (Fig. 4.2). The results show that **1** shows no toxicity to oxic cells over the concentration range tested; that is, the plating efficiency of the cells incubated in the presence of **1** does not differ significantly from the control cells in the absence of **1**. These results are in accord with other reports from this laboratory showing that various cobalt, copper and platinum porphyrin complexes are also non-toxic to oxic cells.^{4,5}

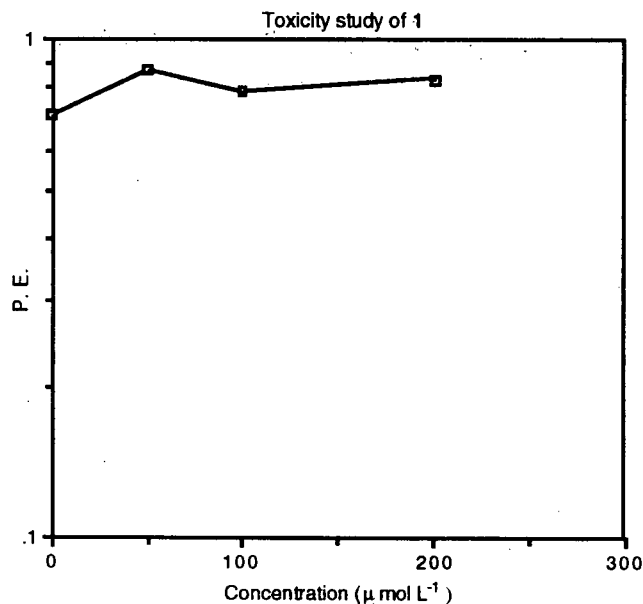


Figure 4.2: Toxicity study of complex 1 (50 - 200 $\mu\text{mol L}^{-1}$) in CHO cells (oxic conditions).

4.4 DNA Binding

4.4.1 Plasmid binding

The complexes 1, 2, and *Cis*-platin (a gift from Bull Laboratories, Australia) were dissolved in solutions of Tris-EDTA (1 mmol L^{-1} EDTA and 10 mmol L^{-1} Tris-HCl, pH 8) and were stirred for one hour (2.5 mmol L^{-1} , 2.5 mmol L^{-1} , and 1 mmol L^{-1} respectively). Plasmid DNA, pBlu, (ScaI/incarized pBluescript® II KS+/-, Stratagene, 20 μL) was added to each sample and Tris-EDTA was added to make a final volume of 100 μL . Each sample was shaken, spun in the refrigerated centrifuge (4 °C) and was incubated at 37 °C for 24 hours. Each sample was then pipetted onto a Sephadex column (G50, coarse, Pharmacia) and was centrifuged (3000 rpm, 5 min) to remove any unbound metal complex. The eluent (DNA with bound compound) was treated as follows. To one aliquot (25 μL) was added a sample buffer, React 3 (3 μL , Gibco), and the restriction enzyme, EcoR1 (2 μL , Gibco); a second

aliquot was treated similarly, but with the restriction enzyme, BamH1 (2 μ L, Gibco). The solutions were shaken, centrifuged (4 $^{\circ}$ C), and incubated for one hour at 37 $^{\circ}$ C. A loading dye (0.25% Bromophenol Blue, 0.25% xylene cyanol, 30% glycerol, 69.50% H₂O; 6 μ L) was added to each digest and 12 μ L of each solution was loaded onto a gel (1% agarose). The gels were set up in electrophoresis tanks and were run for 90 minutes at 100 eV.

4.4.1.1 Electrophoresis gels

The separated DNA fragments on each gel were visualized as bands with a UV light box and a Polaroid picture was taken. The resulting negative was analysed with a video densitometer and the relative amounts of DNA in the individual bands were determined as the integrated optical density (IOD) of the bands. The binding factor is defined as the IOD of the parent band divided by the IOD of the parent band plus the additional cut bands (two bands) (eq 4.2). Therefore the more binding there is, the less EcoR1 or BamH1 can cut the DNA and the greater the Binding Factor (B. F.).

$$\text{Binding Factor} = \frac{\text{Intensity of Parent Band}}{\text{Total Intensity}} \quad [4.2]$$

The results (Fig. 4.3) indicate that there is much less binding of **1** ([**1**] = 0.8 mmol L⁻¹, B. F. = 0.027) or **2** ([**2**] = 0.8 mmol L⁻¹, B. F. = 0.174) than *Cis*-platin ([*Cis*-platin] = 2 μ mol L⁻¹, B. F. = 0.781) at the BamH1 binding sites of the plasmid DNA. When **1** and **2** are compared, there is much less relative binding of complex **1**. This difference in binding indicates that the coordination environments of Ru are probably important biologically. The more labile DMSO ligands may render complexation of Ru with DNA more facile, while the CO ligand inhibits the interaction of **1** relative to **2**. A Ru-CO linkage in the absence of photolysing radiation or strongly complexing ligands would be expected to interfere with the interaction of **1** with DNA.

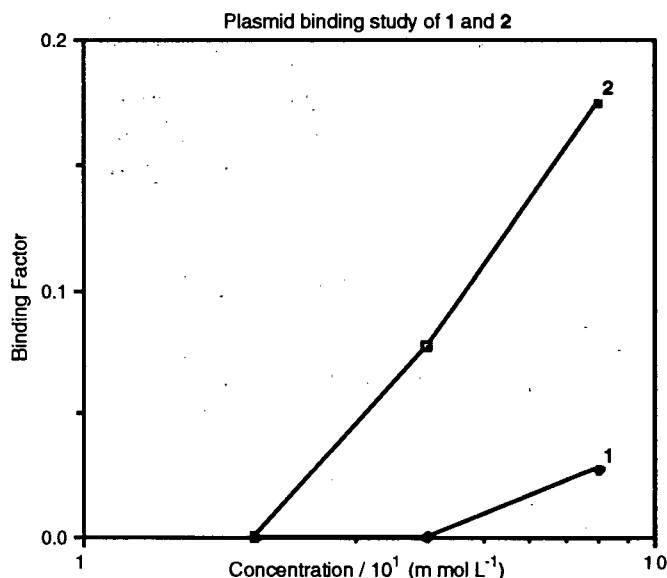


Figure 4.3: DNA binding study of **1** and **2** at or near the BamH1 binding sites of the plasmid DNA.

There was virtually no binding of either complex at or near the EcoR1 binding sites of the plasmid DNA compared to *Cis*-platin ($[Cis\text{-platin}] = 2 \mu\text{mol L}^{-1}$, B.F. = 0.960). The bands observed on the gel could not be identified by the densitometer as the resolution was too poor. This experiment was repeated several times with higher initial concentrations of **1** and **2** (2.5 mmol L^{-1}) but the results were inconsistent.

4.4.2 The Damaged DNA Affinity Precipitation Assay (DDAP)[†]

The DDAP was first used to isolate proteins which recognized DNA that had been damaged by exposure to X-rays.⁶ The assay has since been used to examine the proteins that recognize DNA damaged by *Cis*-platin; these were identified as “high mobility group”

[†] All the buffers used in this assay are described in reference 11.

proteins (HMG).⁷ The functions of these proteins is not clear but they may have important roles in maintaining the structure of DNA, in transcription, and in the binding of H1 histones to DNA.⁸ The HMG proteins that bind specifically to DNA damaged by *Cis*-platin have been identified as HMG1 and HMG2.^{9,10} A modified DDAP assay¹¹ was therefore used to compare the interaction of **1** with DNA to that of *Cis*-platin.

The assay involved the use of double and single stranded calf thymus DNA bound to a cellulose bead (Sigma, 100mg) which was incubated (24 hours at 37 °C in a test tube) in 1 mmol L⁻¹ solutions of the **1**, **2** and *Cis*-platin in buffer A. Each test tube was wrapped in foil to prevent UV light from damaging the DNA. After incubation the solutions were centrifuged (600 rpm, 3 min) and the supernatant was removed; they were then washed with buffer B (4 mL), centrifuged (600 rpm, 4 min), and the supernatant was removed. This was repeated until the solution was clear and colourless, to ensure the complete removal of any complex not already bound to DNA. The solutions were then washed with buffer C (5 mL), centrifuged (600 rpm, 5 min), and the supernatant was decanted. To each solution was then added Tris-HCl (2 mL) and these mixtures were then vortexed. To 30 µL of each solution was added HMG protein (30 µL), and these mixtures were then shaken on ice and centrifuged in the refrigerated centrifuge (4 °C); the residue was then washed with buffer D (1 mL) five times and with buffer E (1 mL) twice and were then dried. Loading buffer (0.5 mmol L⁻¹ Tris-HCl (pH 6.8), 10% sodium dodecyl sulfate, 0.1% Bromophenol Blue, 20% glycerol, 5% 2-mercaptoethanol; 15 µL) was added to each solution which was then boiled for 2 minutes and loaded (10 µL) onto the electrophoresis gel (12.5% polyacrylamide). After electrophoresis was complete the gel was stained with Coomassie blue (0.1%) (Sigma) and was destained with 10% ethanol / 7.5% acetic acid.

4.4.2.1 Results of the damaged DNA precipitation

The presence of the protein band on the gel indicated whether or not there was an interaction between the complex bound to DNA and HMG. The assay was carried out twice and, in each case, interaction with the HMG protein occurred only when *Cis*-platin was bound to the double-stranded DNA cellulose. Both Ru(II) porphyrin complexes, **1** and **2**, have been shown to interact with isolated DNA (see Section 4.4.1) but from the results of this assay, the HMG protein has not been found to recognize this interaction. Other Ru complexes, e.g. *trans*-RuCl₂(DMSO)₄ and *cis*-RuCl₂(DMSO)₄, have been shown to interact with the HMG protein when bound to DNA-cellulose, the former more than the latter.² The way that the *trans* complex binds to DNA is already known to be the same as for *Cis*-platin (see Section 1.5.2).^{12,13}

4.5 Radiosensitization

The assay for radiosensitization¹⁴ is similar to the assay used for toxicity (Section 4.3). Sterile Ru porphyrin solutions in glass "duck vessels"² were stirred for 1 hour. Hypoxic conditions were maintained by passing oxygen-free nitrogen (Linde Speciality Gas, Union Carbide) over the shaking porphyrin solutions (Orbit Shaker) which were kept in a constant temperature (37 °C) bath. CHO cells in 1mL α(+/-) (3×10^6 mL⁻¹) were added to each solution and sparging with nitrogen continued for 1 hour at 37 °C. After the incubation period, the vessels were chilled to 0 °C for at least 5 min prior to irradiation, and filtered air was briefly bubbled through two solutions (a and b) to produce radiobiologically aerobic conditions. The other three solutions (c, d, and e) were kept under a stream of nitrogen. The cells in each vessel were irradiated in turn by being placed in a flask of ice water on the head of the X-ray source (Philips, 250 kV, 0.5 mm Cu). The radiosensitizing apparatus was set up as described by earlier work⁴ and calibrated using a Victoreen model 500 Precision Electrometer (typical radiation dose-rate was 4.5 Gy/min).

Samples (1 mL) of cells were removed after every 2 Gy increment (a and b) and every 5 Gy increment (c, d and e), and placed into dilution tubes containing 9 mL $\alpha(-/-)$ at 0 °C. In like manner to the toxicity studies (Section 4.4), the cells were centrifuged, and resuspended in 10 mL $\alpha(-/-)$. Cells were counted using a Coulter counter (after diluting 2 mL cell solution into 10 mL PBS), plated in Petri dishes, and incubated for 7 days, after which time the cell colonies were stained with methylene blue and counted.

The survival curves presented were generated by plotting the surviving fraction (SF) versus dose received (eq 4.3):

$$SF = \frac{\text{P. E. (at dose D)}}{\text{P. E. (at zero dose)}} \quad [4.3]$$

4.5.1 The radiosensitizing ability of 2

The radiosensitizing ability of a complex is given by the SER value (Sensitization Enhancement Ratio), which is defined as the ratio of radiation doses required to produce a given effect in the absence or presence of the complex (eq 4.4):

$$SER = \frac{\text{Dose without drug}}{\text{Dose with drug}} \quad (\text{at 1\% survival}) \quad [4.4]$$

Complex 2 at 400 $\mu\text{mol L}^{-1}$ has no effect in oxic conditions and shows no radiosensitizing ability at 400 $\mu\text{mol L}^{-1}$ and 800 $\mu\text{mol L}^{-1}$ in hypoxic conditions (Fig. 4.4). Indeed the complex seems to be weakly radioprotecting with an SER value of 0.89. This value is to be compared with those obtained for the free-base porphyrin, $\text{H}_2(\text{TSPP})^{4-}$ (SER value of 1.04)⁴, and for $\text{Na}_3[\text{Co}(\text{TSPP})]$ (SER values of 1.08 and 2.30)^{4,15}, which show that these complexes have some radiosensitizing ability. DMSO has been shown to act as a radioprotector at much higher concentrations (2.0 mol L^{-1} and 3.5 mol L^{-1}).^{16,17}

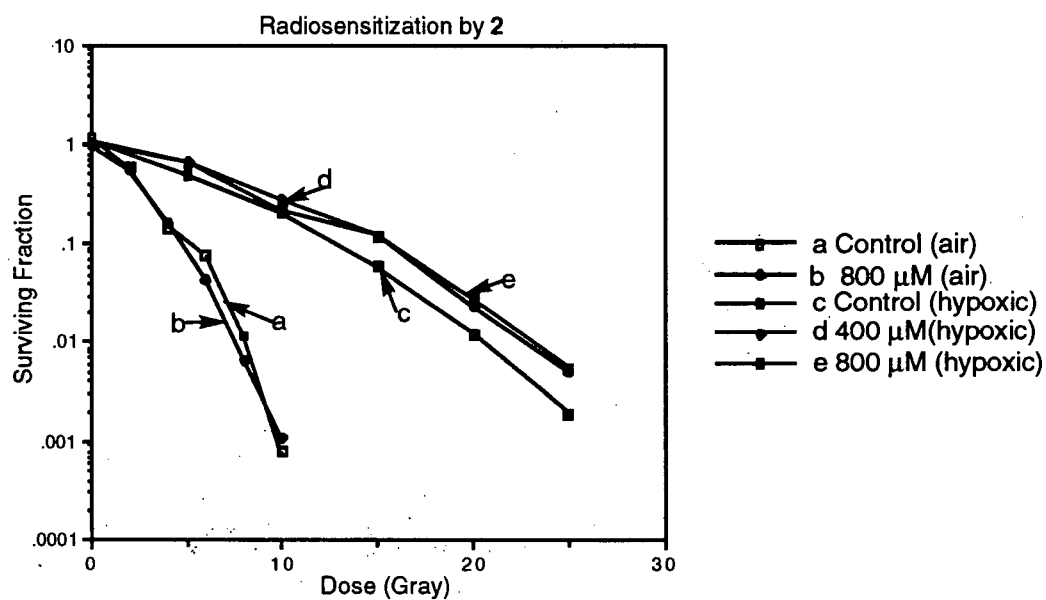


Figure 4.4: Survival curve for radiosensitizing by 2 in oxic and hypoxic CHO cells.

The experiment was only performed with complex 2 as there was not enough of complex 1 remaining to be tested.

4.6 References

- (1) Matthews, J. B.; Adomat, H.; Skov, K. A. *Anti-Cancer Drugs* **1993**, 4, 463.
- (2) Yapp, D. T. T. Ph. D. Thesis, University of British Columbia, 1993.
- (3) Moore, B. A.; Palcic, B.; Skarsgard, L. D. *Radiat. Res.* **1976**, 67, 459.
- (4) Meng, G. G. Ph. D. Thesis, University of British Columbia, 1993.
- (5) Ravensbergen, J. A. M. M. Sc. Thesis, University of British Columbia, 1993.
- (6) Boothman, D. A.; Bouvard, I.; Hughes, E. N. *Cancer Res.* **1989**, 49, 2871.
- (7) Hughes, E. N.; Engelsberg, B.; Billings, P. C. *J. Biol. Chem.* **1992**, 267, 13520.
- (8) Bradbury, E. M. *The HMG Chromosomal Proteins*, E. W. Johns (ed.); Academic Press: London, 1982, p 89.
- (9) Scovell, W. S.; Muirhead, N.; Kroos, L. R. *Biochem. Biophys. Res. Comm.* **1987**, 142, 826.
- (10) Hayes, J. J.; Scovell, W. M. *Biochim. Biophys. Acta* **1991**, 1088, 413.
- (11) Marples, B.; Adomat, H.; Billings, P. C.; Farrell, N. P.; Koch, C. J.; Skov, K. A. *Anti-Cancer Drug Design* **1993**, 9, 389.
- (12) Cauci, S.; Viglino, P.; Esposito, G.; Quadrifoglio, F. *J. Inorg. Biochem.* **1991**, 43, 739.
- (13) Esposito, G.; Cauci, S.; Fogolari, F.; Alessio, E.; Scocchi, M.; Quadrifoglio, F.; Viglino, P. *Biochem.* **1992**, 31, 7094.
- (14) Parker, L.; Skarsgard, L. D.; Emmerson, P. T. *Radiat. Res.* **1969**, 38, 493.
- (15) O'Hara, J. A.; Douple, E. B.; Abrams, M. J.; Picker, D. J.; Giandomenico, C. M.; Vollano, J. F. *Int. J. Radiat. Oncol. Biol. Phys.* **1989**, 16, 1049.
- (16) Chapman, J. D.; Reuvers, A. P.; Borsa, J.; Greenstock, C. L. *Radiat. Res.* **1973**, 56, 291.
- (17) Skov, K. A. *Radiat. Res.* **1984**, 99, 502.

Chapter 5: Conclusions and Suggestions for Future Work

5.1 Retrospective

Various strategies for the synthesis of water-soluble ruthenium porphyrin complexes were discussed in Chapter 3. Following the literature procedure (Section 3.3.1),¹ which no doubt borrows from the classic method of metalloporphyrin synthesis (i.e. thermolysis of $\text{Ru}_3\text{CO}_{12}$), $\text{Na}_4[\text{Ru}(\text{TSPP})(\text{CO})(\text{DMF})]$ (**1**) could indeed be accessed after lengthy reaction time and a tedious work-up procedure. With the new method developed in this thesis work, **1** can be synthesized from a simple Ru(III) starting material after only three hours and with simplified work-up. Metallation was achieved not only with the anionic porphyrin, $\text{H}_2(\text{TSPP})^{4-}$, but also with the neutral species $\text{H}_2(\text{TPyP})$ and $\text{H}_2(\text{TPP})$ as well as with the cationic porphyrin, $\text{H}_2(\text{TMPyP})^{4+}$. This discovery that the Ru(III) precursor, $[\text{Ru}(\text{DMF})_6](\text{OTf})_3$, rapidly inserts into various porphyrin systems, and undergoes *in situ* reduction to Ru(II), to give a corresponding Ru porphyrin species, is a significant inorganic result and establishes a protocol for the synthesis of other Ru porphyrins that will likely be followed by other investigators.

Complete characterization of **1** and $\text{Na}_4[\text{Ru}(\text{TSPP})(\text{DMSO})_2]$ (**2**) was hampered by the lack of solid-state X-ray structural details : all isolated crystals exhibited twinning; in particular, **2** is believed to exhibit O- coordination by the DMSO ligands and a single crystal X-ray diffraction experiment would have shown this conclusively.

In solution both **1** and **2** are suspected to undergo axial ligand exchange (with water), as expected for reasonably labile Ru(II) complexes. For **2**, a ligand exchange process was followed by UV/visible spectroscopy and the process was in fact reversible. Importantly, aggregation phenomena were conspicuously absent for **1** and **2** in solution, a result that contrasts with that observed for the free-base porphyrin, and which may be rationalized by the presence of axial ligands bound to the Ru nucleus. This is consistent with the literature

findings that no metalloporphyrin bearing axial ligands has been found to undergo aggregation.

The biological results reveal that Ru encased in a porphyrin does not accumulate in mammalian cells and bind to DNA as well as Ru does in the form of a simple coordination complex, e.g. *trans*-RuCl₂(DMSO)₄. This indicates that the porphyrin somehow inhibits the passage of Ru across the cell membrane and also prevents binding to DNA. At the very least, both complexes **1** and **2** were found to be non-toxic at the concentration levels tested, and **2** was found to protect the cells from the effects of radiation. That **2** acts as a radioprotector is consistent with the fact that this complex does not contain strongly electron-withdrawing groups such as nitroimidazole that can mimic the effect of oxygen.

5.2 Prospective

The highly significant result from this thesis, the metallation of various porphyrins mediated by [Ru(DMF)₆](OTf)₃, has very important consequences for metalloporphyrin chemistry and raises several questions that need to be addressed. Time did not permit an attempt at the metallation of the other generic porphyrins, such as H₂(OEP), by [Ru(DMF)₆](OTf)₃, and in order to answer the question as to the generality of the method it is imperative that further experiments be performed. A related question is the stability towards reduction of a Ru(III) centre bound to a porphyrin. Can a different porphyrin, maybe more electron-rich, stabilize Ru(III), and what factors generally affect the Ru(II)/Ru(III) redox behaviour? The mechanism advanced in Section 3.3.2 is highly speculative and investigations into the course of the metallation and reduction reactions should be instigated. Is the Ru(III) nucleus first incorporated into the porphyrin ring as seems likely, or is another process at work? Possible techniques to monitor more carefully the metallation may include UV/visible and IR spectroscopy (if a carbonyl species is formed), or ESR spectroscopy.

Further work on the coordination chemistry of **1** and **2** will lead to new Ru chemistry in aqueous solution. Both **1** and **2** have potential applications in catalysis, both in aqueous media (for example, in the Water Gas Shift reaction¹) and in organic phases as Ru complexes have a well established activity in catalytic oxidations, hydrogenations, and hydroformylations.^{2a,b} It is also of interest from a fundamental view to examine the substitution chemistry of both complexes. What other ligands can coordinate? Several ligands suggest themselves as candidates, such as phosphines, amines, and nitroimidazoles (*vide infra*).

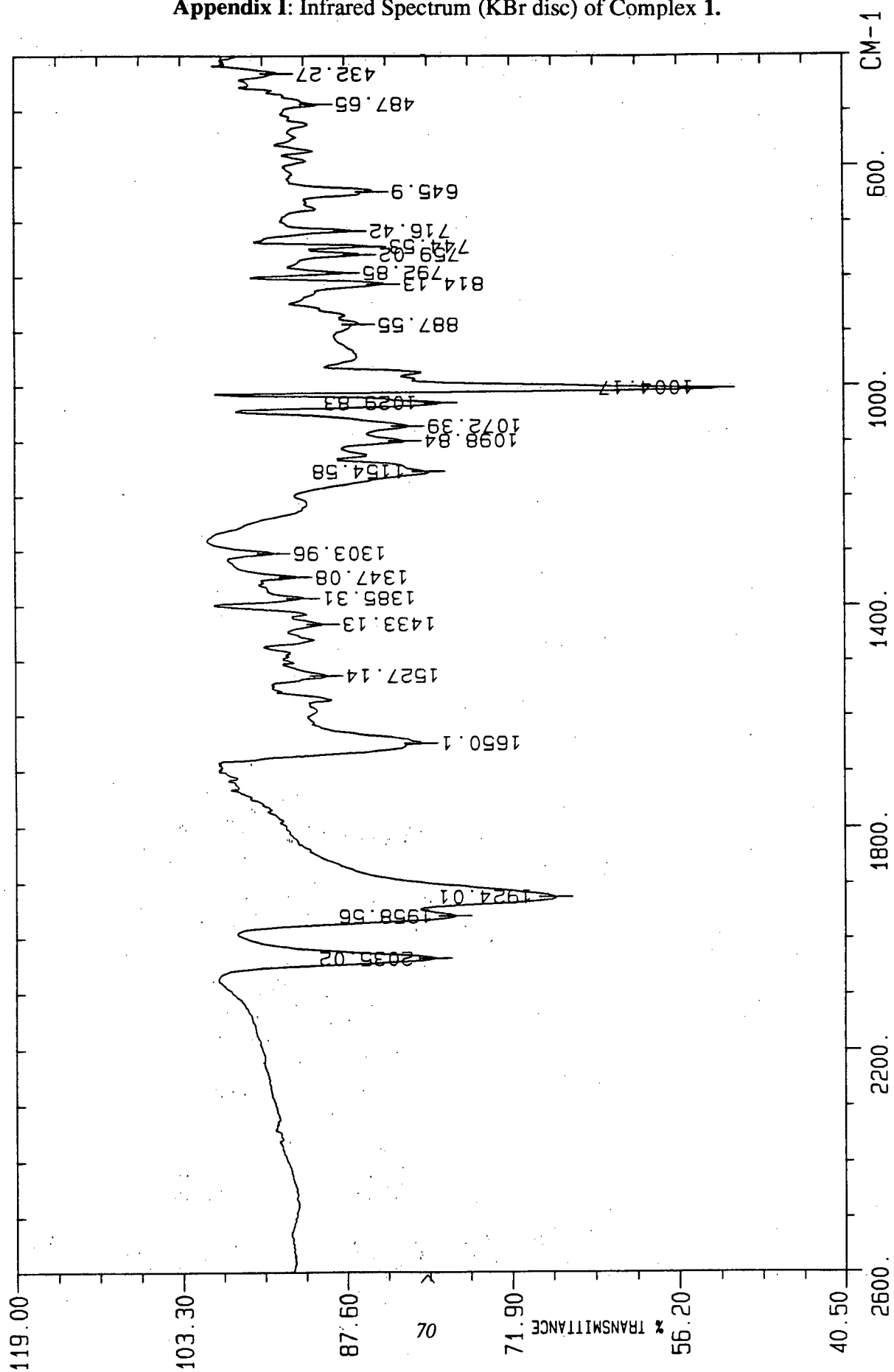
The biological results are a bit disappointing, particularly as one of the stated aims of this thesis was to develop water-soluble Ru porphyrin complexes as radiosensitizers. To improve the radiosensitizing potential of Ru bound porphyrins the attachment of a nitroimidazole group either directly to the Ru nucleus or as a *meso*-substituent of the porphyrin ring may be required. As regards cellular accumulation, in hindsight it is probably unreasonable to expect significant passage of **1** or **2** across a cell membrane when both complexes bear four formal negative charges. Prior work has established enhanced uptake for cationic porphyrin systems.³ Another alternative might be the replacement in **1** and **2** of the four Na⁺ counter-ions by K⁺, which could be accomplished simply by an ion-exchange resin; this could yield more favourable results, especially as mammalian cells possess a well-recognized mechanism for K⁺ uptake.

In summary, it is clear that the fundamental aspects of Ru porphyrin chemistry, to say nothing of its opportunities for biological applications, continue to offer a great deal of potential.

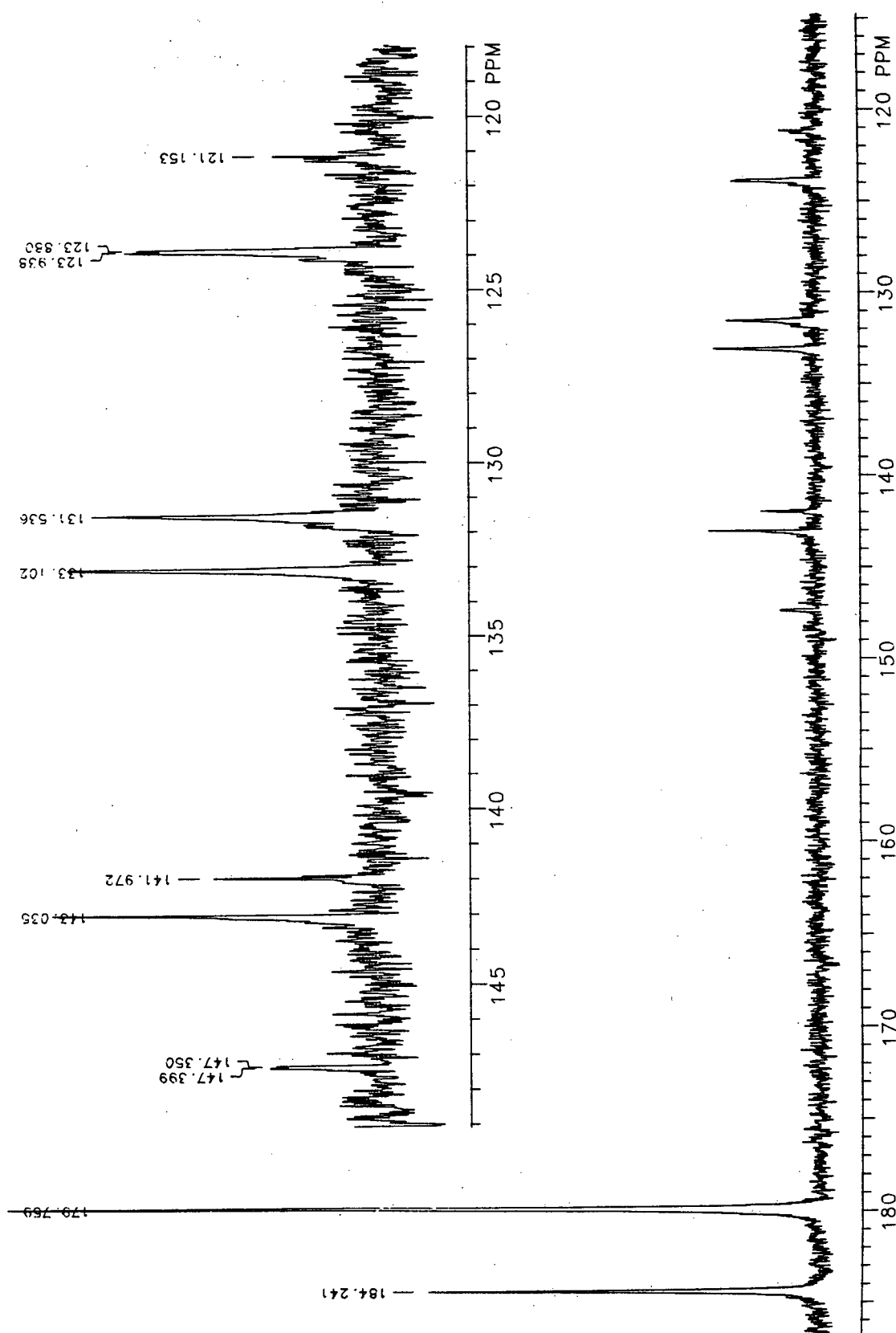
5.3 References

- (1) Pawlik, M.; Hoq, M. F.; Shepherd, R. E. *J. Chem. Soc., Chem. Commun.* **1983**, 1467.
- (2) (a) Mlodnicka, T.; James, B. R. In *Metalloporphyrin Catalyzed Oxidations*; F. Montanari and L. Casella, Eds.; Kluwer Academic: Dordrecht, 1994; p 121.
(b) Parshall, G. W.; Ittel, S. D. *Homogeneous Catalysis*; 2nd ed.; John Wiley & Sons, Inc.: New York, 1992.
- (3) Meng, G. G. Ph. D. Thesis, University of British Columbia, 1993.

Appendix I: Infrared Spectrum (KBr disc) of Complex 1.



Appendix II: $^{13}\text{C}\{^1\text{H}\}$ NMR Spectrum of $\text{Ru}(\text{TSPP})(^{13}\text{CO})(\text{DMF})_4$.



Appendix III: Solutions Used for the Biological Tests.

1. α -Media

An alpha-modification of Eagle's minimum essential media (MEM, Gibco) was used in three different forms (α (+/+), α (+/-), α (-/-)) depending on the needs of the experiment. One packet of an α -media powder and 10,000 units of Penstrep antibiotic (Gibco) were added to 10 L of double distilled water and the solution was stirred for 2 hours at room temperature to make α (-/-).

The α (+/-) medium was made by adding foetal bovine serum (10%, 50 mL) to α (-/-). Stock solutions were sterilized by filtration (Nalgene filter, 0.22 micromillipore), and stored at 4 °C.

Foetal Bovine serum (10%, Gibco) and NaHCO_3 were added to α (-/-) medium and the pH was adjusted to 7.3 (4 mol L⁻¹ NaOH) to produce the α (+/+) medium. All solutions of media were sterilized by filtration (Nalgene filter, 0.22 micromillipore) and the filtered solutions were stored at 4 °C. Each batch was tested for contamination by incubating the solutions for 1 week.

2. Phosphate Buffer Saline solutions (PBS).

NaCl (160 g), KCl (4 g), Na_2HPO_4 (23 g) and KH_2PO_4 (4 g) were dissolved in distilled water (20 L), and the solution sterilized by filtration (Nalgene filter, 0.22 micromillipore). The solution was stored at room temperature and was cooled before use when required.

3. Tris -HCl buffer.

This solution was prepared from Trizma-HCl (Sigma), and the pH of the solutions adjusted to 7.5-8.00 using 4 mol L⁻¹ NaOH. Stock solutions were diluted as required.